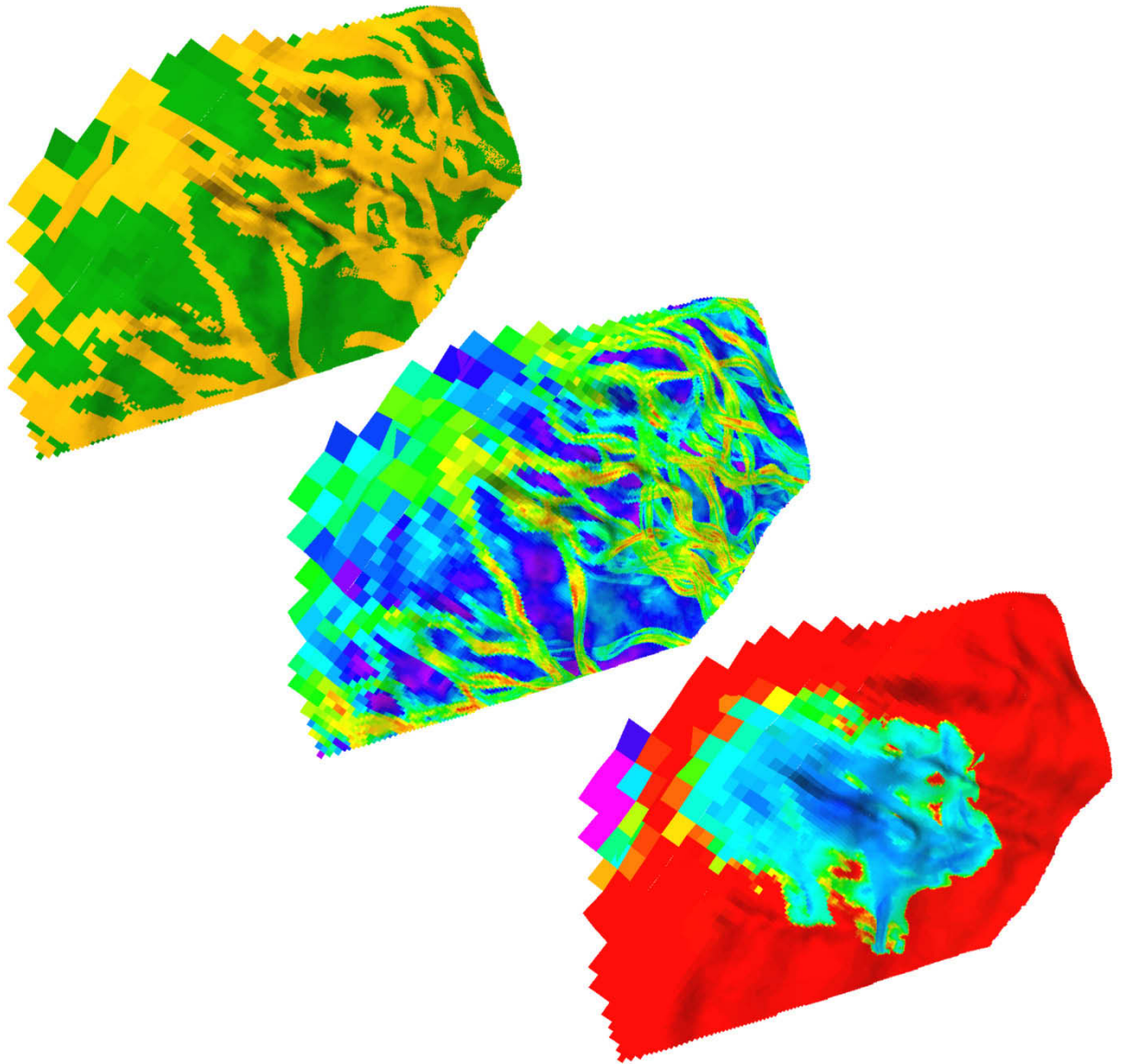# Managing the Interdisciplinary Requirements of 3D Geological Models

Sarah Jane Riordan
Australian School of Petroleum
University of Adelaide
March 2009

THE UNIVERSITY OF ADELAIDE
AUSTRALIA
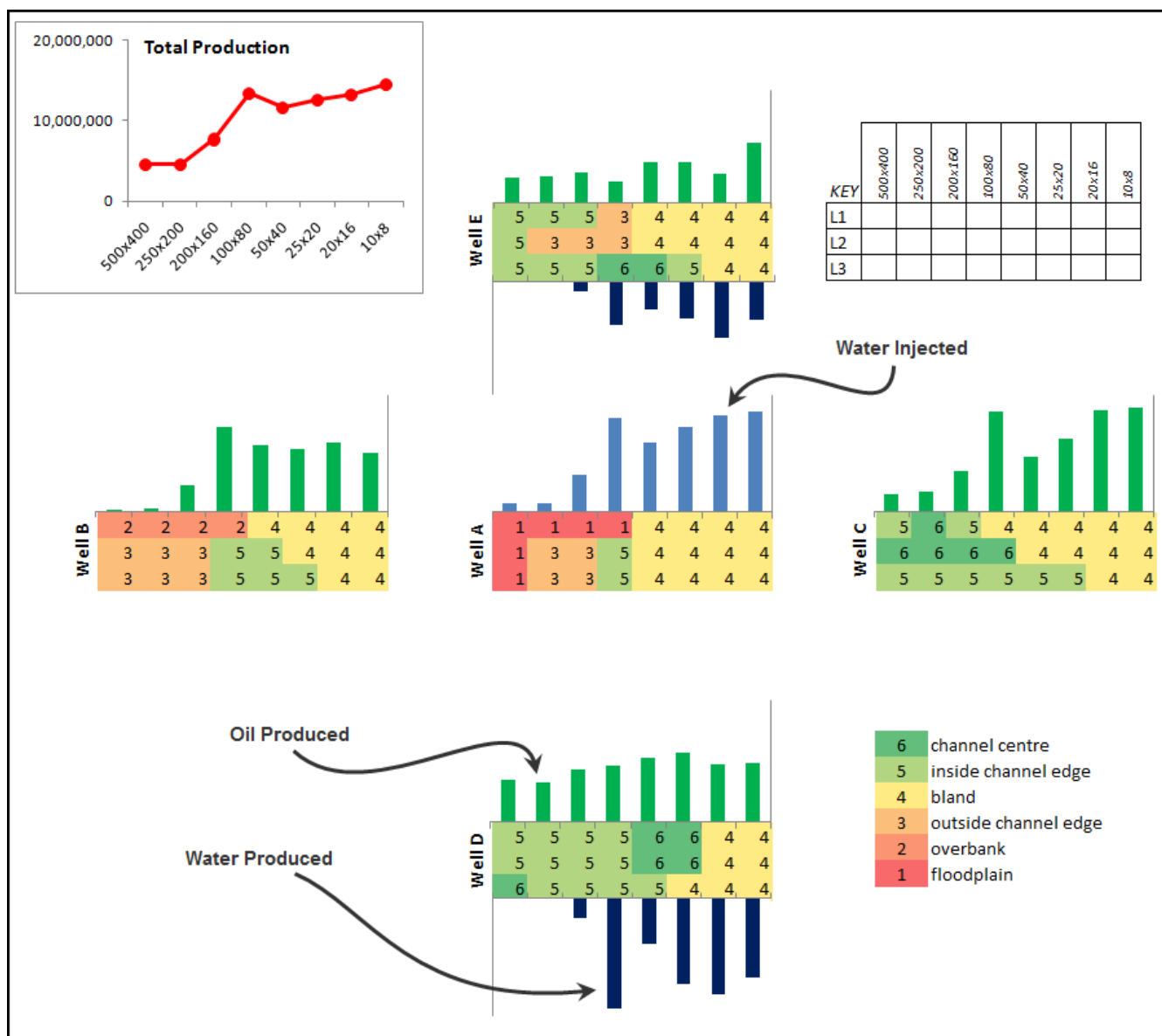SUB CRUCE LUMEN

ASP
Australian School of Petroleum

Figure 6.29. Channel proximity to wells. Realization 9, SQ100-25 scenario. This realization provides an excellent example of how upscaling beyond half the width of the channel can influence the results of reservoir simulation. The injector well (A) is located in an area of poor porosity in the base model. However, as the grids are upscaled the edge of the channel shifts, to the point that in the 200 x 160 grid the well is located on the inside edge of the channel. This is the first grid that produces any water in wells D and E, and significant increases in production are seen in wells B and C compared to the smaller grids.
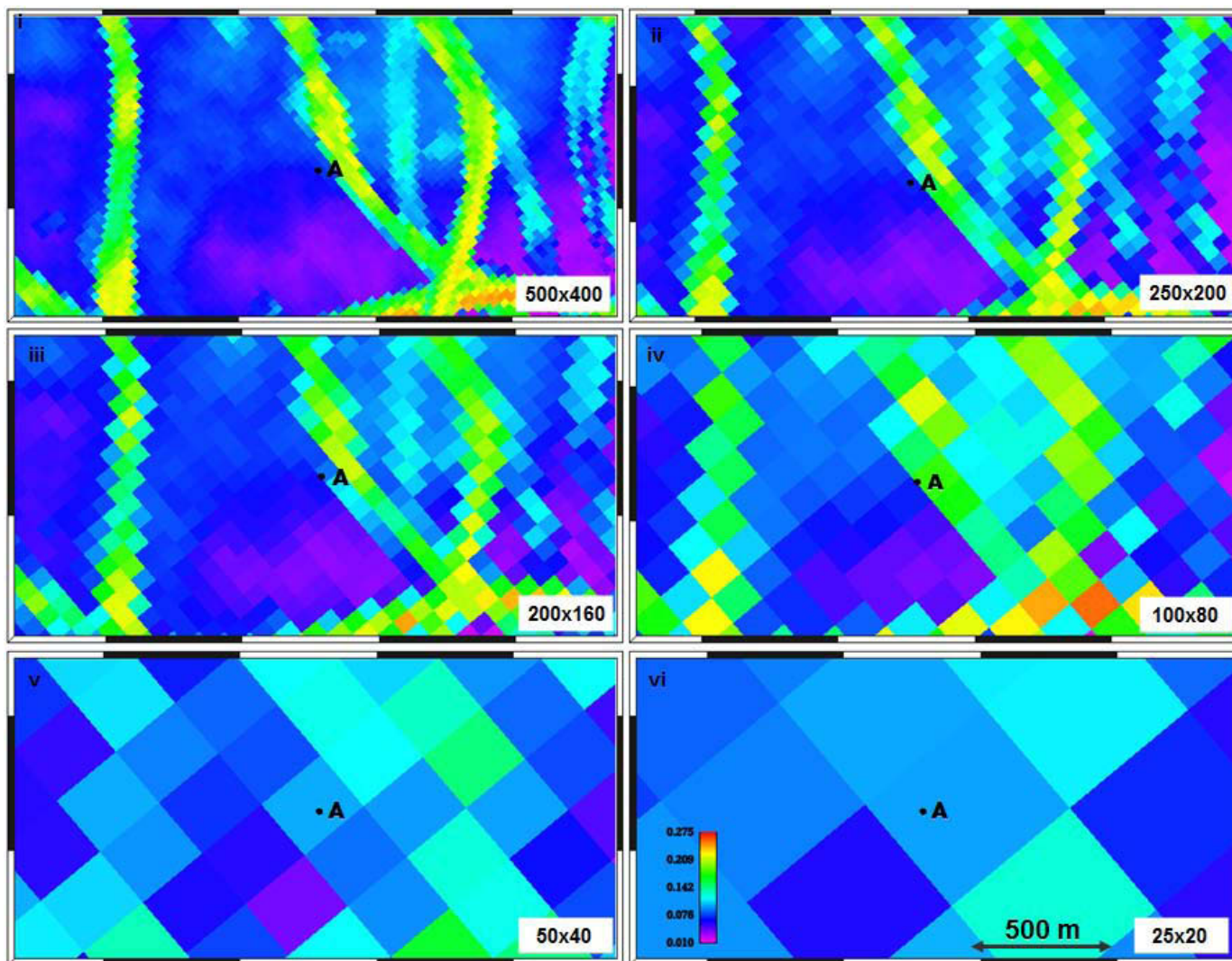
Figure 6.30. Detail of porosity grid around Well A, Realization 9, SQ100-25 scenario. As the grid is upscaled the position of Well A relative to the channel changes. On the 100 x 80 grid the well is within the high porosity streak associated with the channel. In the 50 x 40 and 25 x 20 grid the channels are no longer distinguishable As can be seen in Figure 6.29, the amount of water injected into Well A increases dramatically in the 100 x 80 grid compared to the 200 x 160 grid. This increase is also reflected in the productivity of the producing wells, all of which penetrate channel facies.
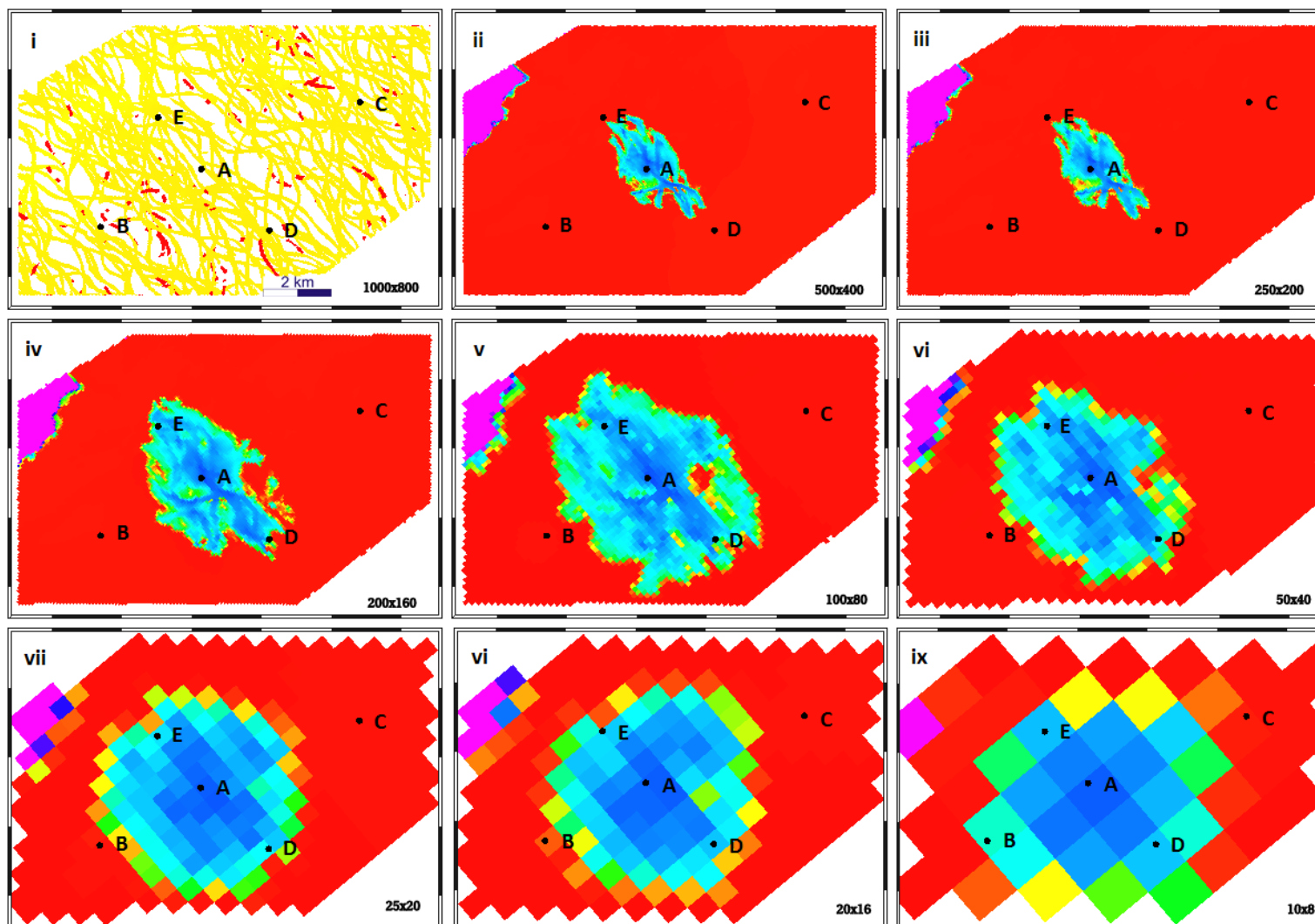
Figure 6.31. Reservoir simulation, water influx. SQ100-25 scenario, realization 9, Layer 3 of 3 at 20 years. Note the step-wise changes in water influx as the cell sizes increase. In Figures ii and iii the channel widths are half the width of the cell (iii) or less (ii) (x direction). As the cell size approaches the channel width (iv) and exceeds it, the water influx pattern changes significantly, resulting in a clear change in ultimate production as the cell sizes get larger. In the 100 x 80 grid, the well is located within the porosity streak associated with the channel (Figure 6.30).
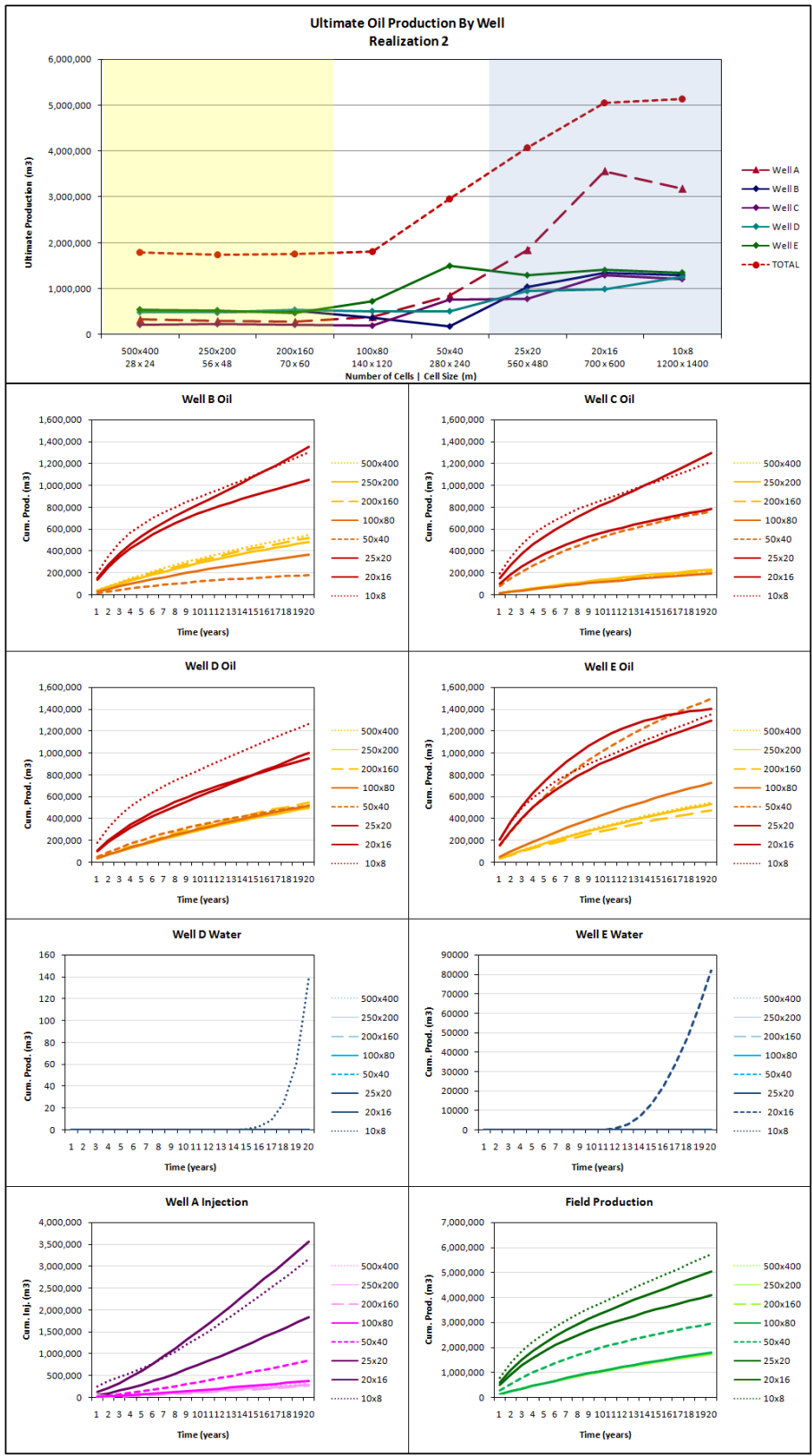
Figure 6.32. Production profiles of Realization 2. SQ100-25 scenario. None of the wells penetrate channel facies in this realization.
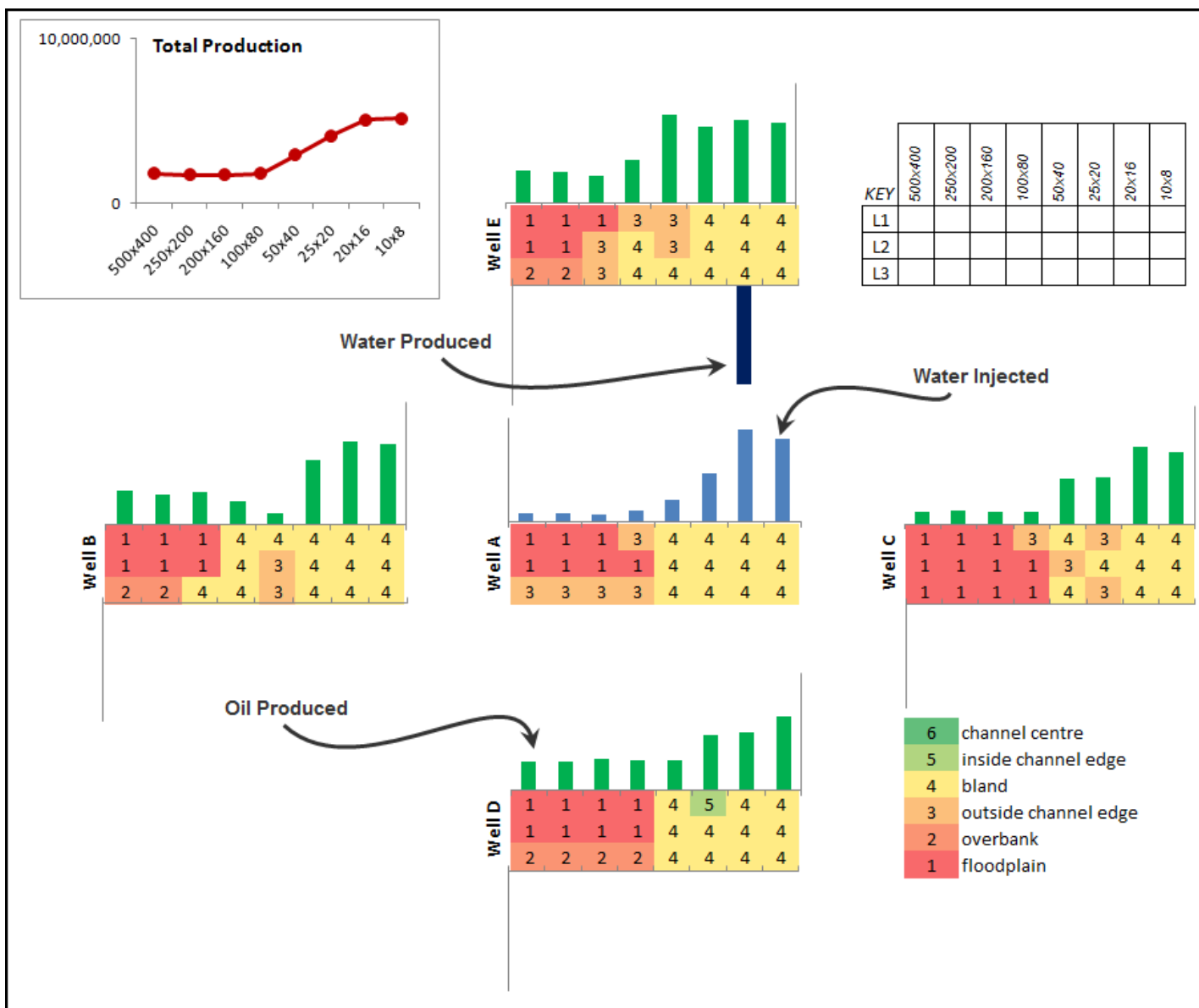
Figure 6.33. Channel proximity to wells. Realization 2, SQ100-25 scenario. None of the wells penetrate the channel facies in this realization. Significant injections and production only occurs once the grids have been upscaled to the point that there is very little contrast in the porosity grid.
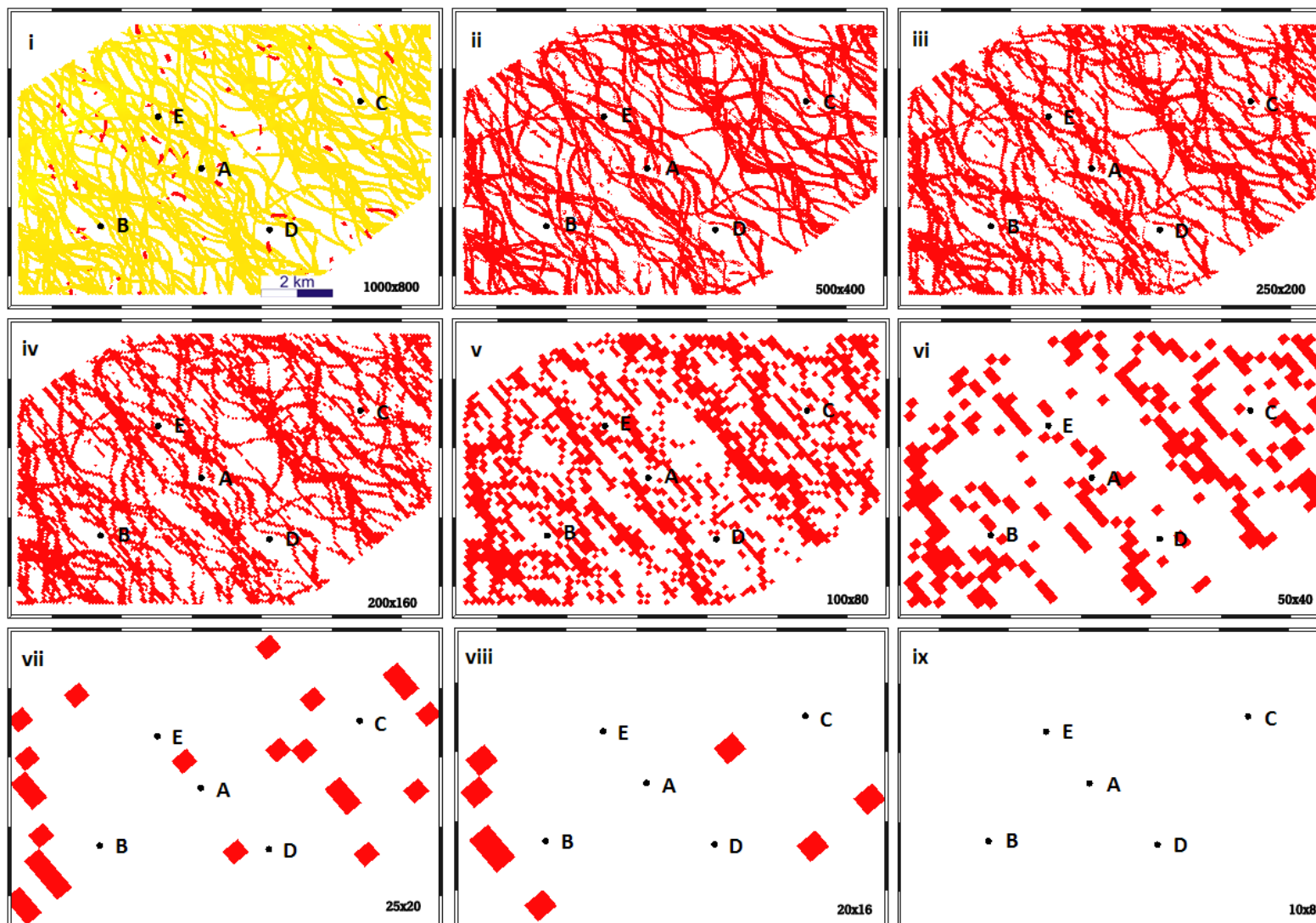
Figure 6.34. Channel connectivity, Realization 2, SQ100-25 scenario. All layers are visible. In this output style, yellow channels are connected to each other and to at least one of the wells, while red channels have no connectivity with the wells. Thus, for this realization, none of the wells are connected to the channels. As can be seen in Figure 6.32 and Figure 6.33 this realization has low production and poor water influx.
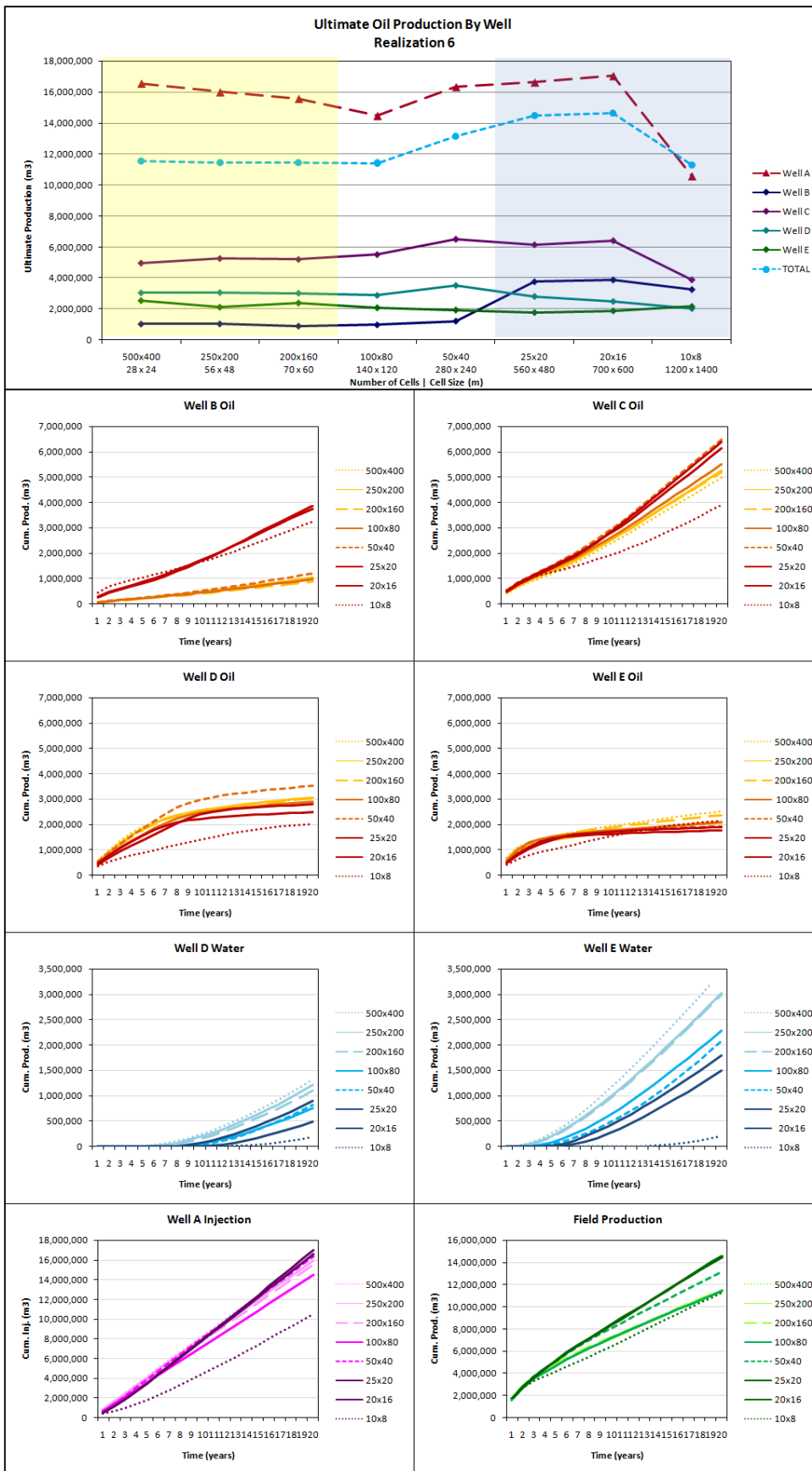
Figure 6.35. Production and injection profiles for Realization 6, SQ100-25 scenario. This realization has one of the best oil recovery profiles. The trend of the field recovery is very similar to that of Realization 2—a flat profile until the cell size is approximately 1.5 times the channel width. This pattern is reflected in all the wells. The water production profiles change between the 200 x 160 and the 100 x 80 grids—the point at which cell size exceeds channel width.
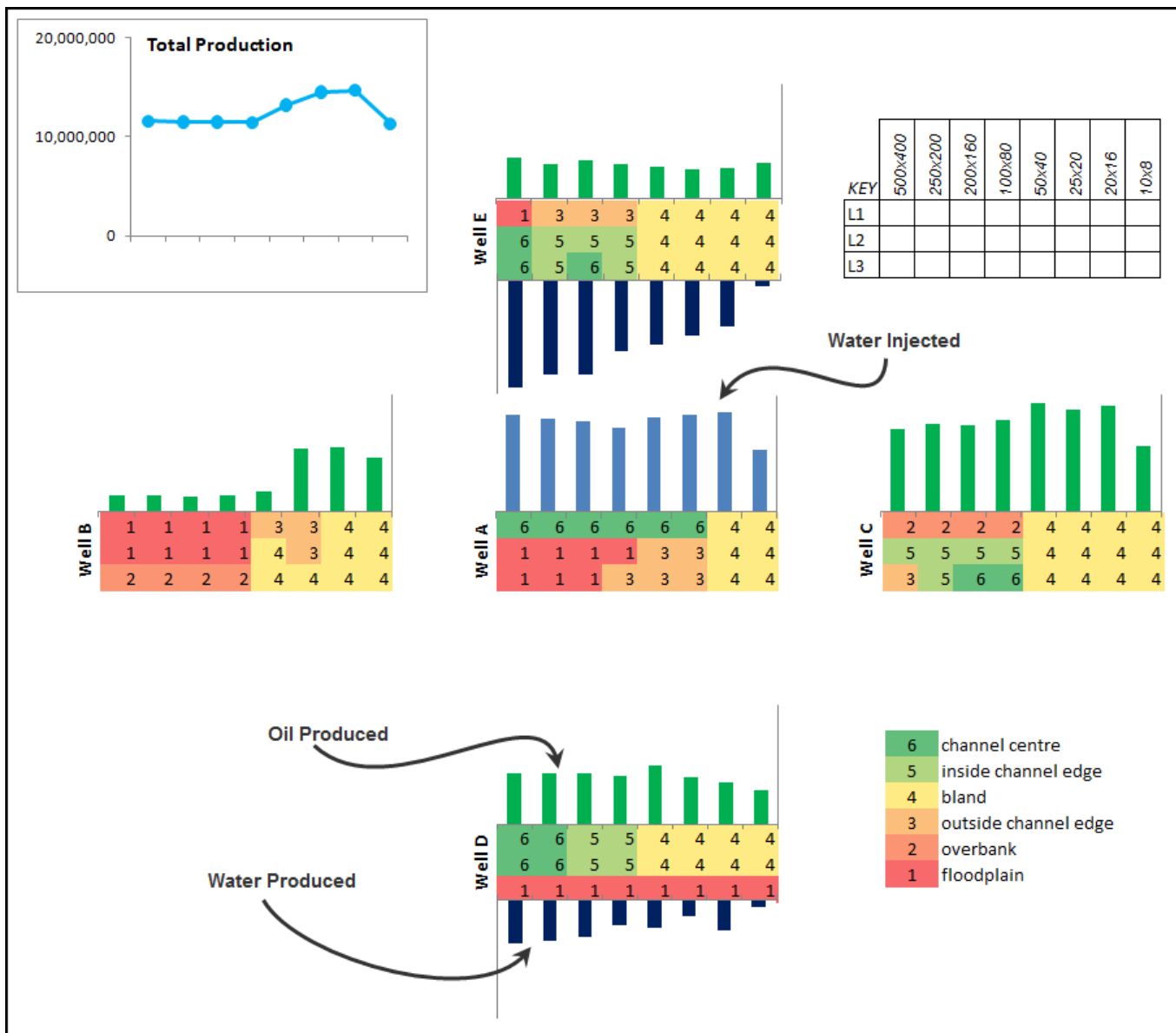
Figure 6.36. Channel proximity to wells. Realization 6, SQ100-25 scenario. Production from this realization is high as the injector and three producers penetrate the centre of channels in at least one layer of the model.
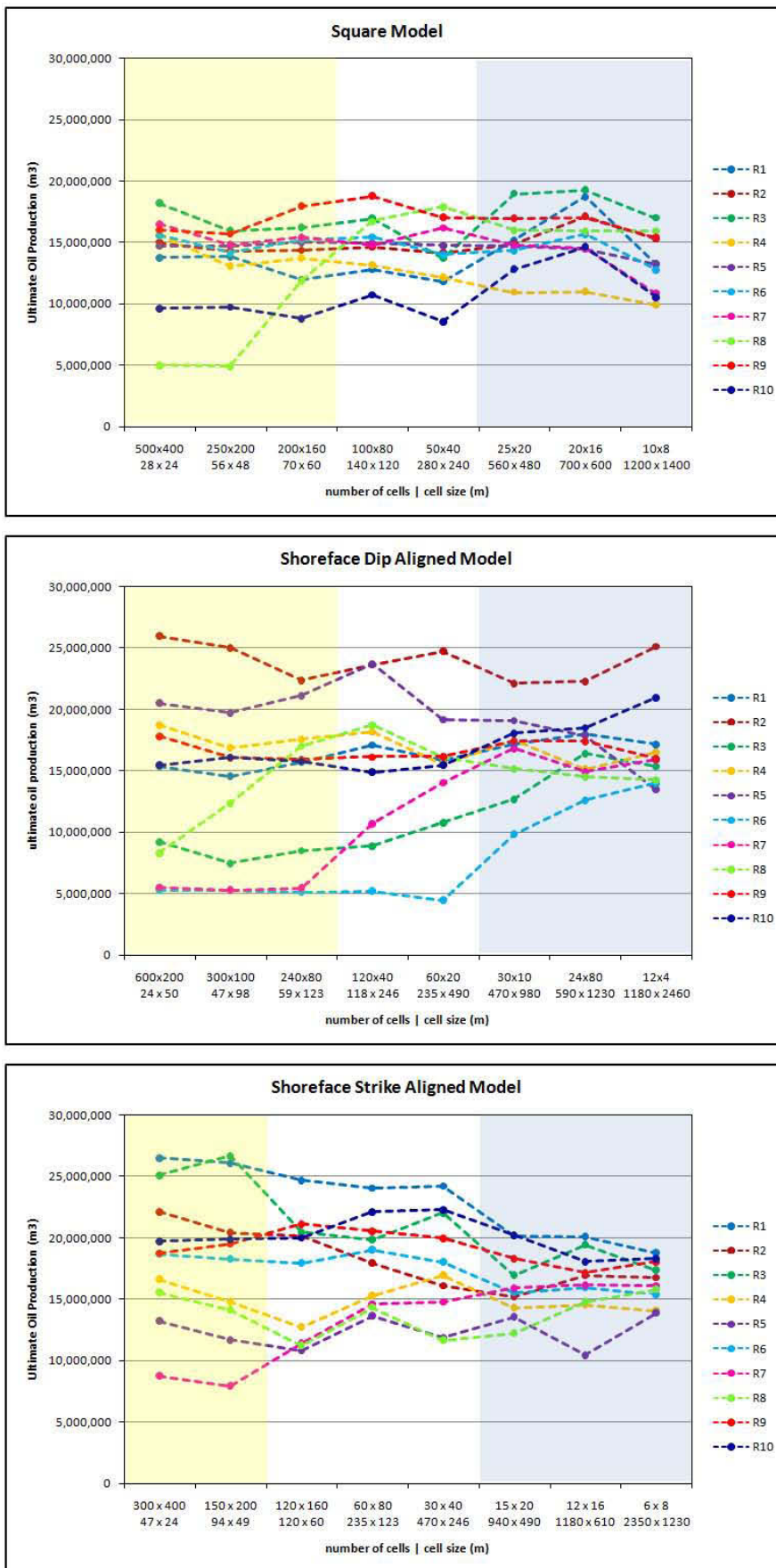
Figure 6.37. Total field production, 100-50 scenario. Grids where grid cells are smaller than channel width are highlighted by the yellow tint. The blue-grey tint highlights grids where there are three or fewer cells between the injector and at least one of the producers.
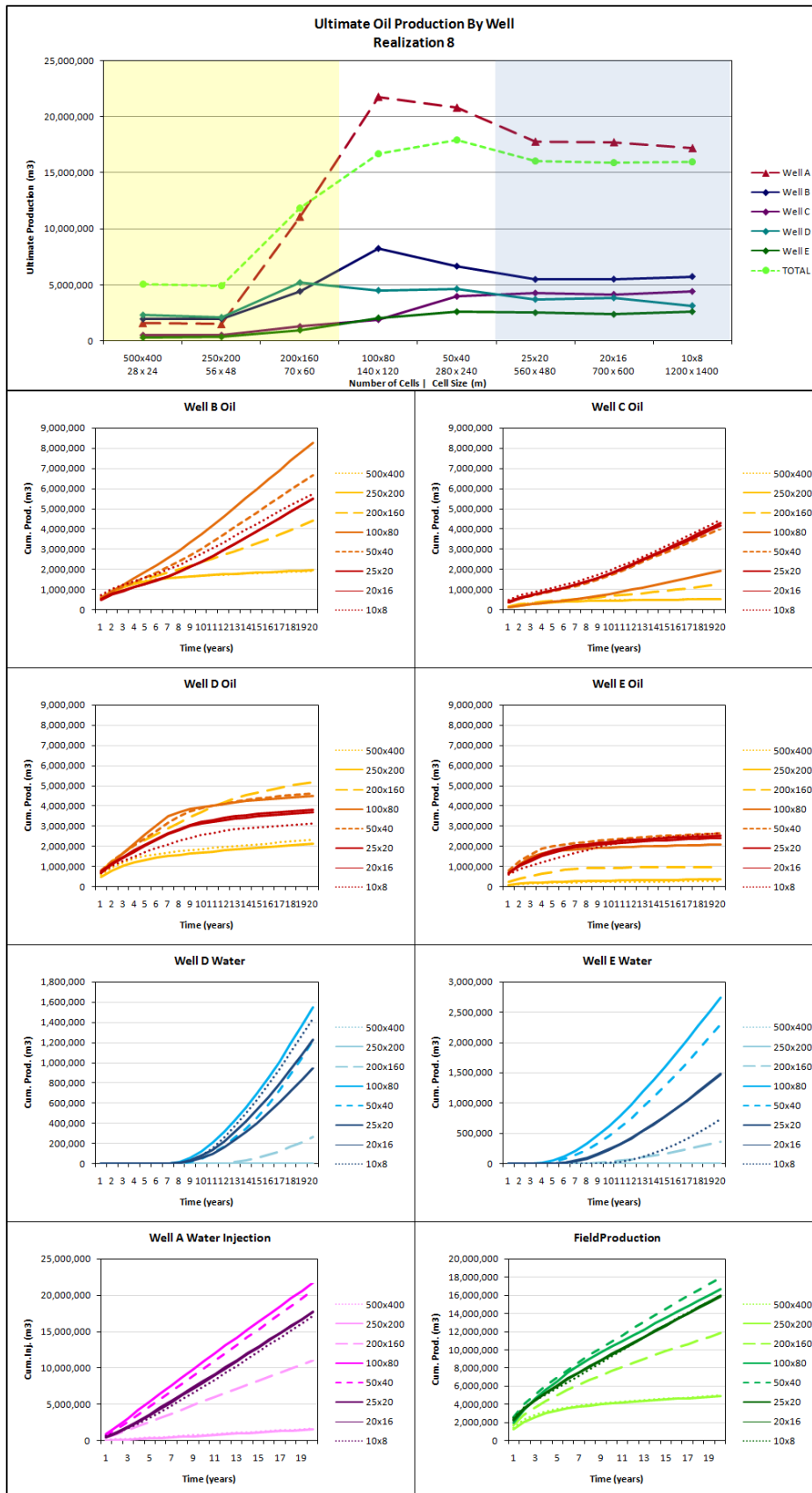
Figure 6.38. Production profiles of SQ100-50 scenario, Realization 8. This realization shows a dramatic increase in total field production once the cell size exceeds half the channel width. All wells show this behaviour, suggesting that the primary cause for this performance is the behavior of the injector Well A. As seen in Figure 6.39, this suggests that Well A is located in poor quality reservoir close to a channel edge. Well E, which has the poorest production and least response to the changes at Well A is likely to also be located in poor quality reservoir.
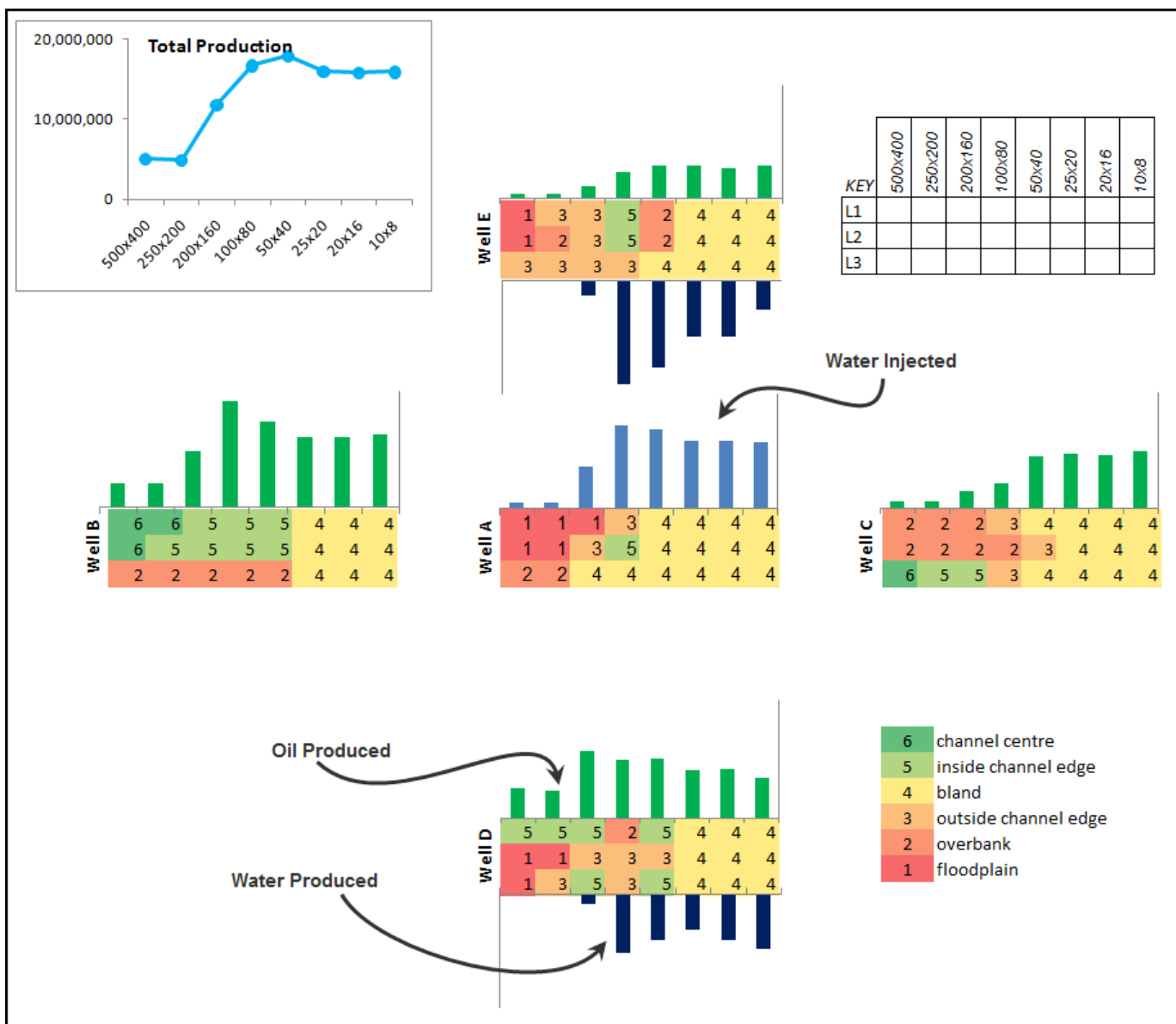
Figure 6.39. Channel proximity to wells. SQ100-50 scenario, Realization 8. Porosity trends near the well bores. This indicates that Well A does not penetrate any channels in the base model and minimal injection occurs until upscaling begins to alter the porosity distribution of the grids.
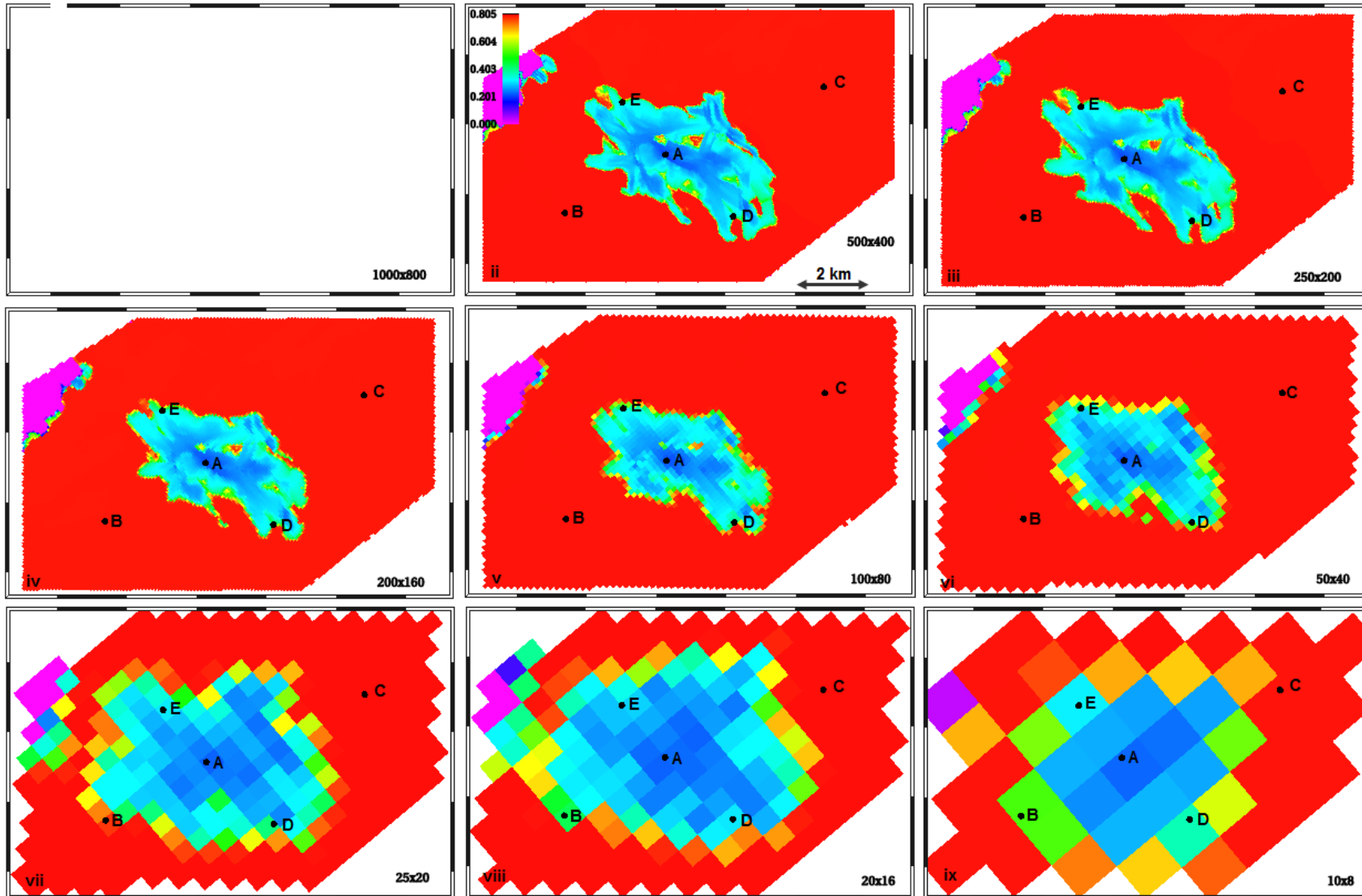
Figure 6.40. Oil saturation at the end of 20 years of production, SQ100-50 scenario, Realization 2. The channels are the same width as the cells in the 50 x 40 grid. In this grid, the distribution of injected water is similar to that of the finer grids but the boundaries of the channels are no longer visible.
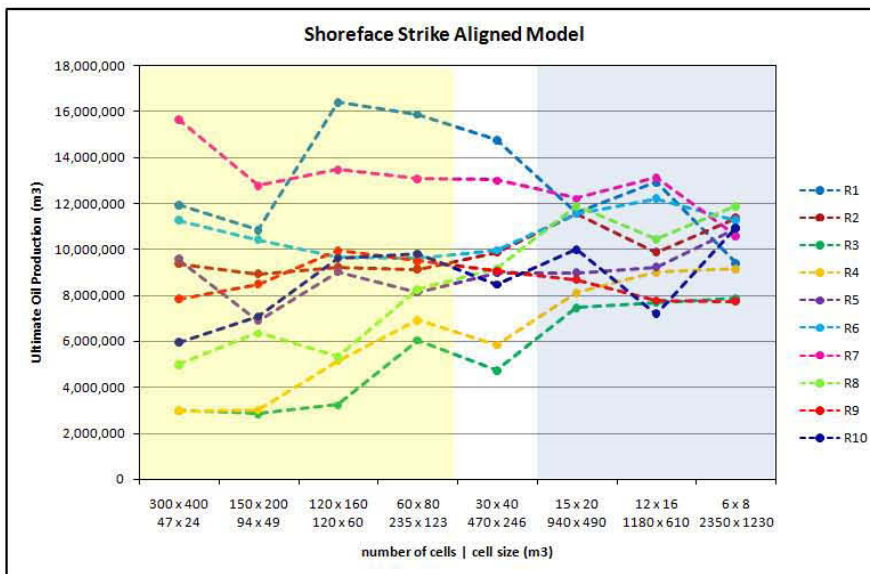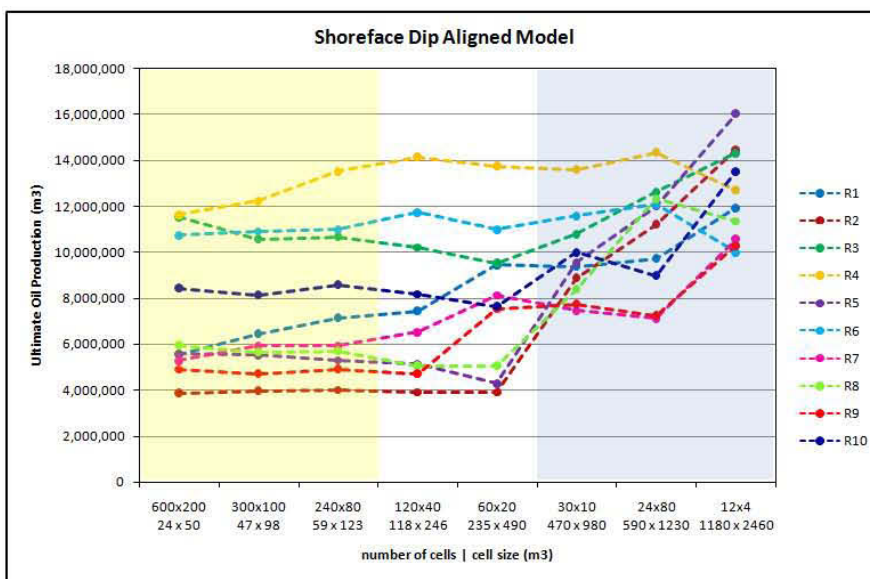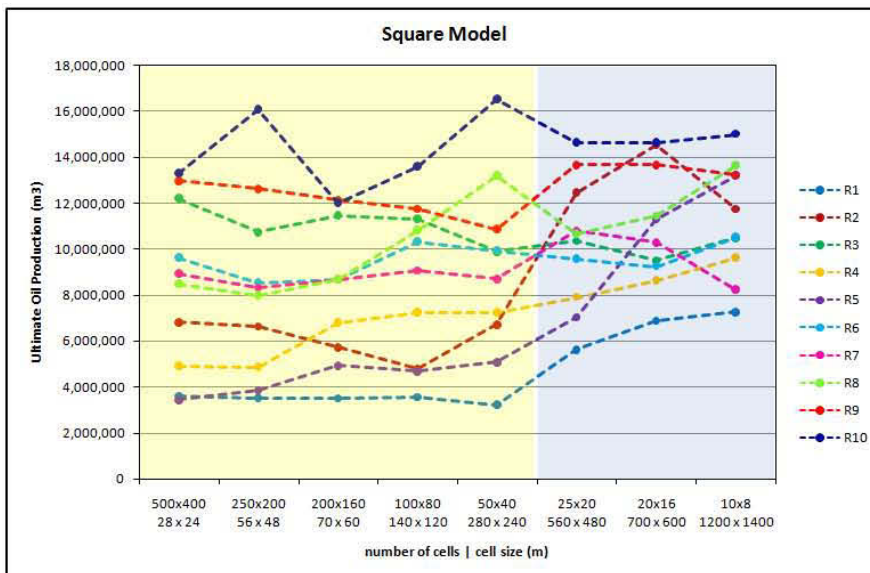
Figure 6.41. Total field production, 280-25 scenario. The square and SDA grids a good for examining changes to simulation results when the grids are less than half the channel width, as in these models there are three grids that have cells less than half the channel width. The extremely stable results seen in the SDA grid are due to the fact that in all the realizations the wells are located either within channels or away from channels. The square grid and the SDA grid are both good at preserving the channel width and placement as the x-axis of these grids (narrowest face of the cells) is approximately normal to the channel orientation. The large changes in the SQ280-25 Realization 10 and SSA Realization 1 are due to the fact that one of the wells is located very close to the edge of a channel and as the grids are upscaled there are significant changes in the porosity and kh at the wellbore.
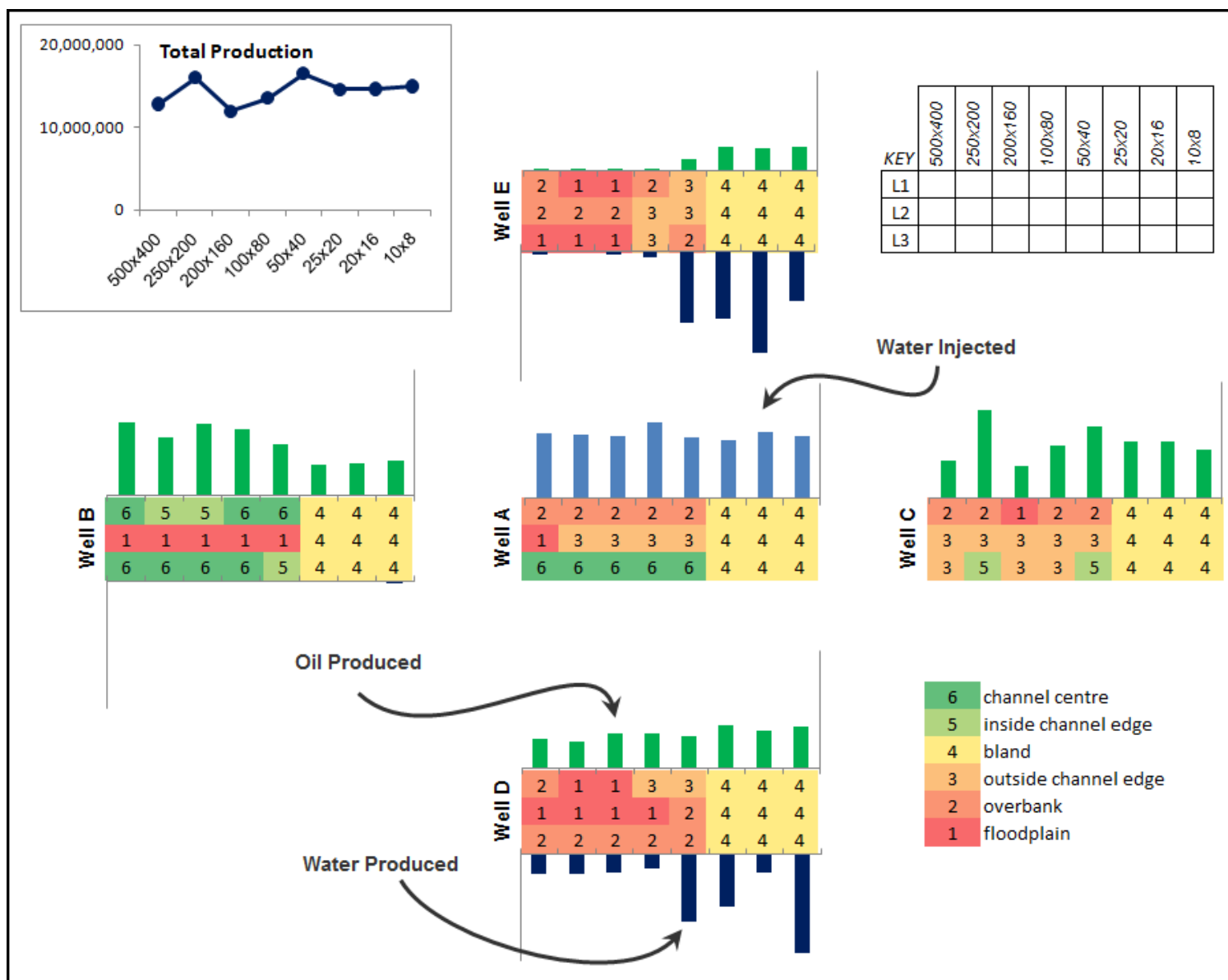
Figure 6.42. Channel proximity to wells. SQ280-25 scenario, Realization 10. The spike in production in the 250 x 200 grid is due to the increased production in well C in this grid. This is the result of the position of the wellbore cell changing from the outside channel edge to the inside edge of the channel. A change in production in the last three cells is also apparent in wells B,C and E. This could be due either to the change in porosity distribution due to upscaling or the unreliable calculations as a result of too few cells in the grid.
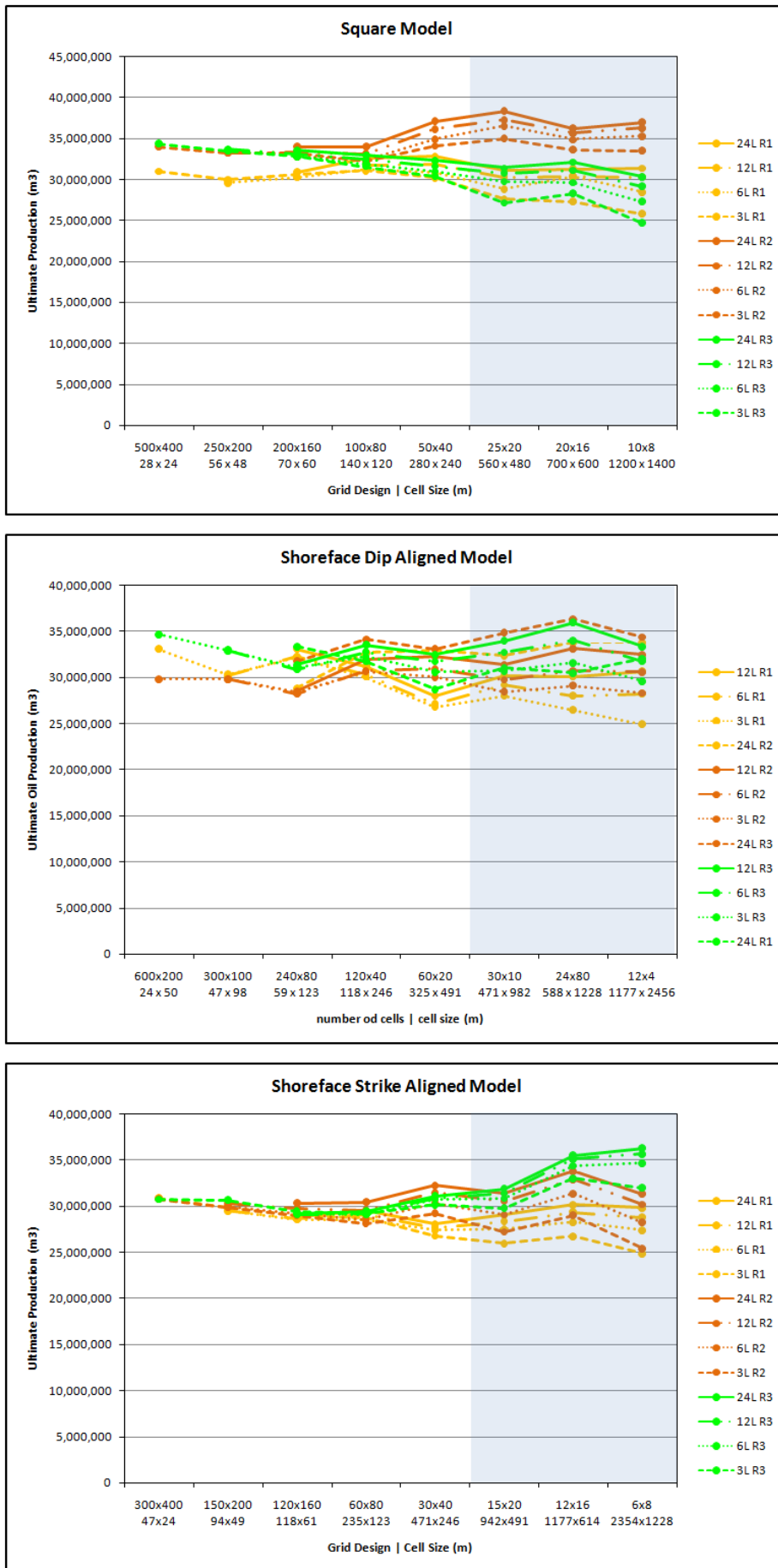
Square Model

Shoreface Dip Aligned Model

Shoreface Strike Aligned Model

Figure 6.43. A comparison of the simulation results for the coast scenario for all grids. The coast scenario consists of a shoreface, channels, offshore and coastal plain facies. For the realizations shown here there is little variation in total field production between realizations or grid designs. There is difference in field production between grids with the same x and y dimensions but difference z (number of layers).
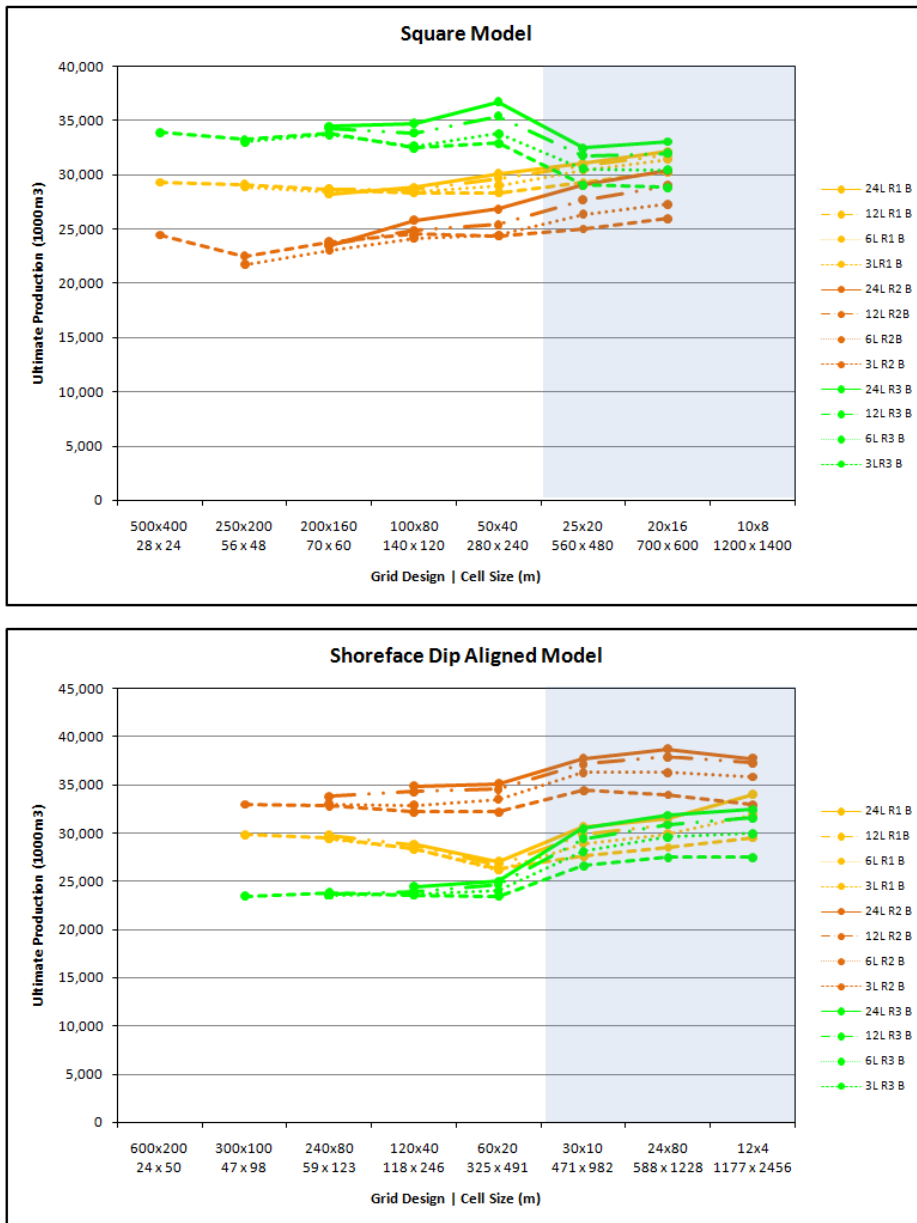
Figure 6.44. Comparison of the simulation results of the beach scenarios for the square and SDA grids.
The beach scenario consists of an offshore, shoreface and coastal plain facies. This scenario shows greater variation of field production between realizations than the 'coast' scenario. There is a similar amount of variation between models as the grids are vertically upscaled.
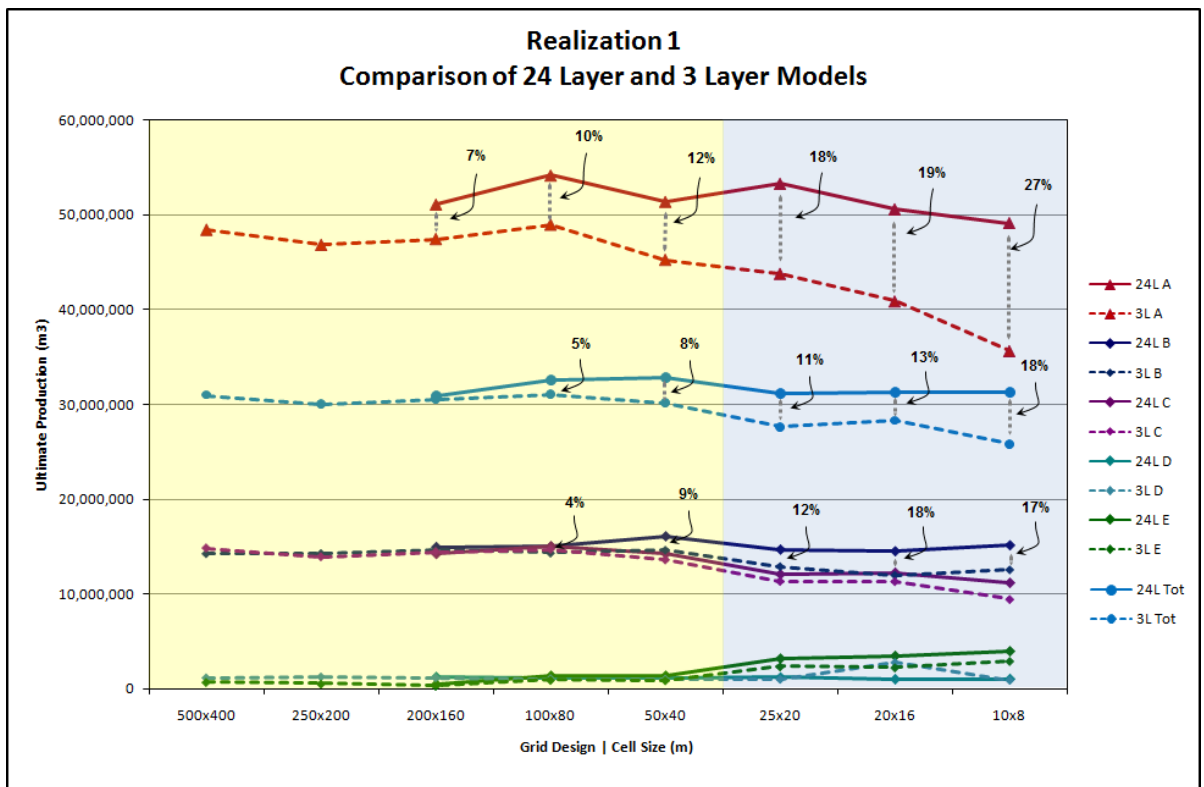
Figure 6.45. Ultimate production. Square grid, coast scenario. This graph compares the ultimate production or injection for each well of the 24-layer grid and the 3-layer grid. It shows that the 24 layer and 3-layer grids produce similar trends in ultimate production as the grids are upscaled. This chart indicates that vertical upscaling has a greater influence on the amount of water injected than on the amount of oil produced. This highlights the need to examine more than one factor when assessing the potential impact of upscaling.
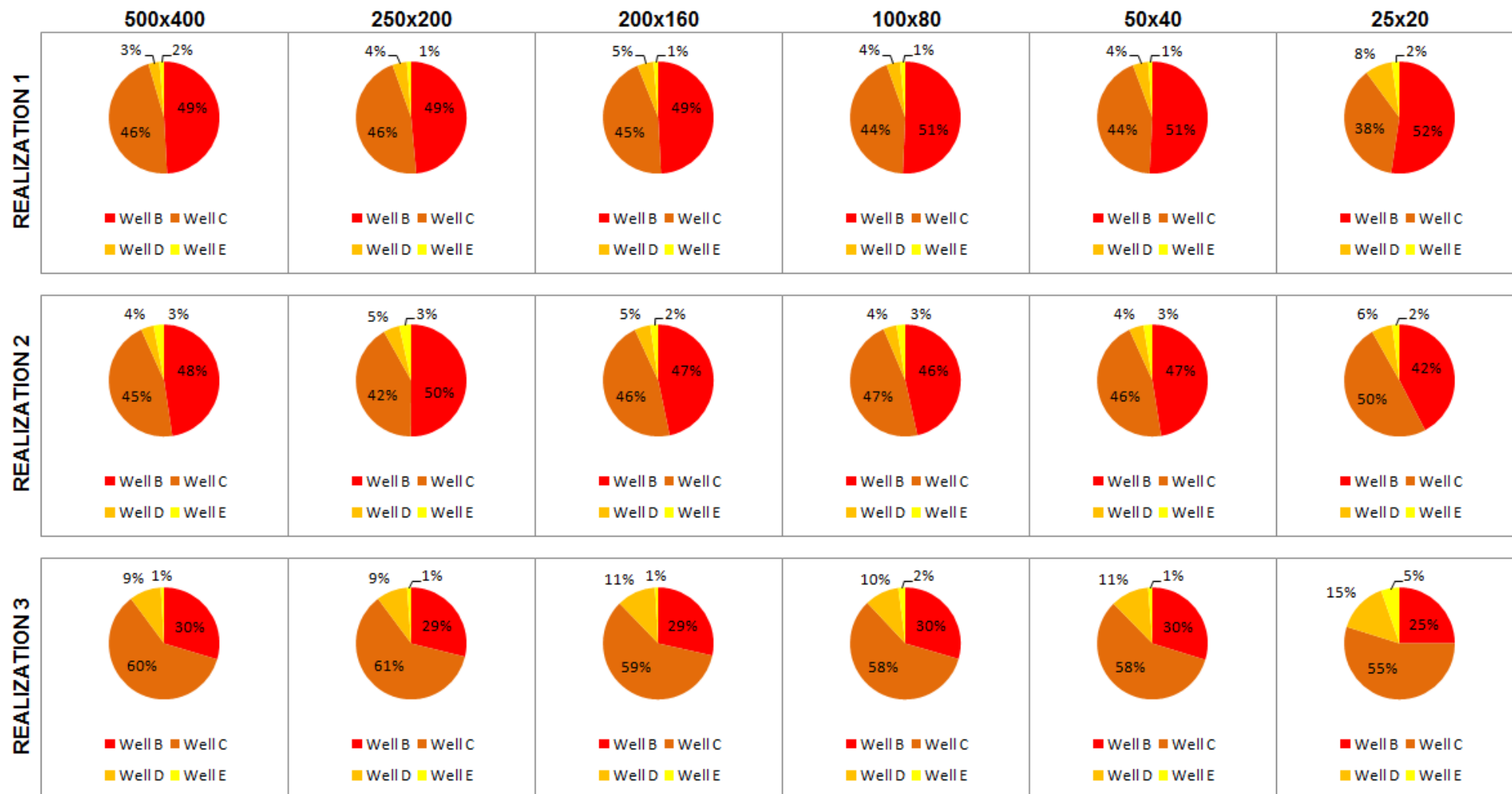
Figure 6.46. Relative contribution of wells to total field production - beach scenario, square grid. These pie charts highlight the consistency of the performance of the wells in this scenario as the grids are upscaled.
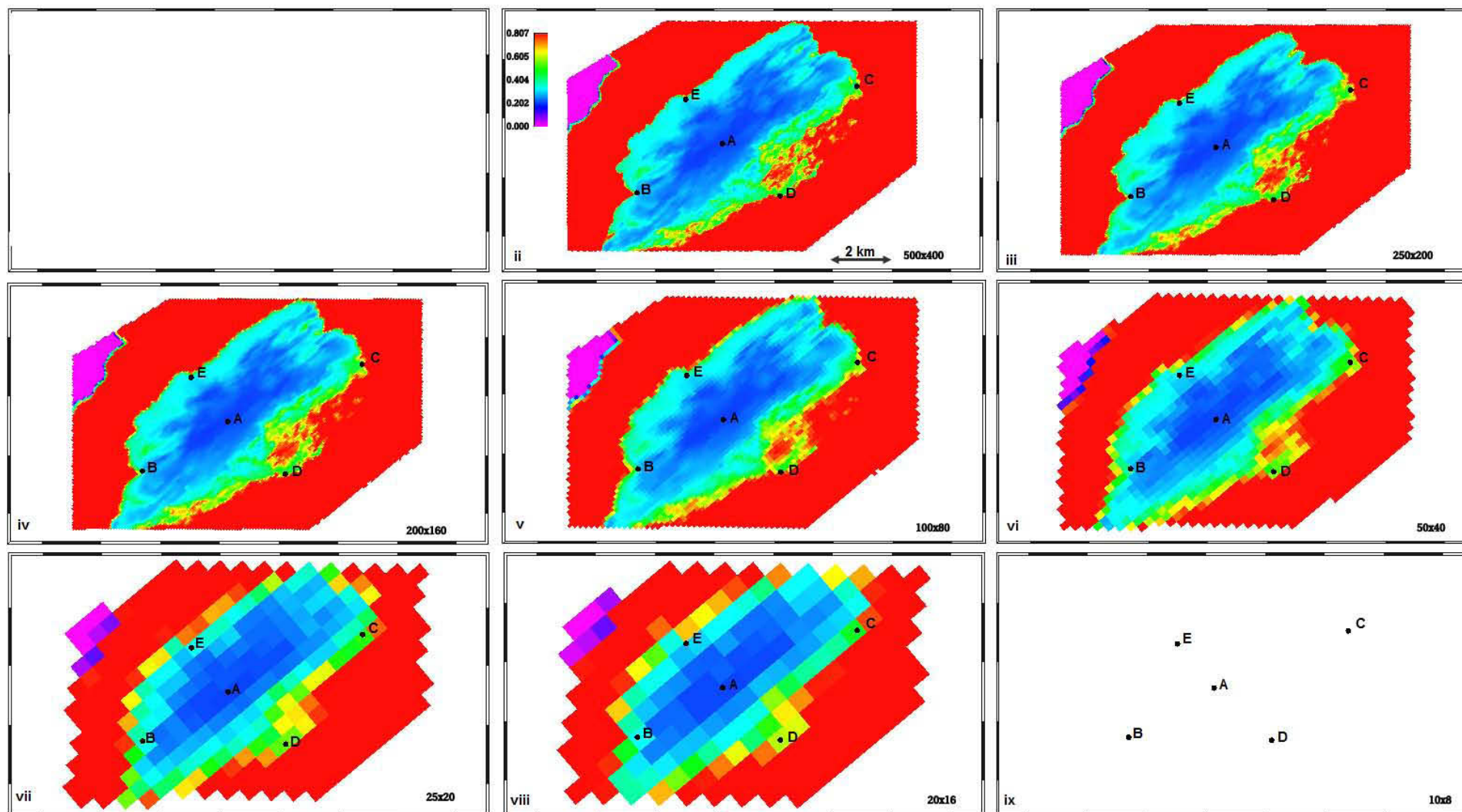
Figure 6.47. Oil saturation after 20 years of production - beach scenario, square grid - Realization 2. Upscaling has little impact on the distribution of the water flood until in this scenario. The water flood pattern is recognizable in all grids.
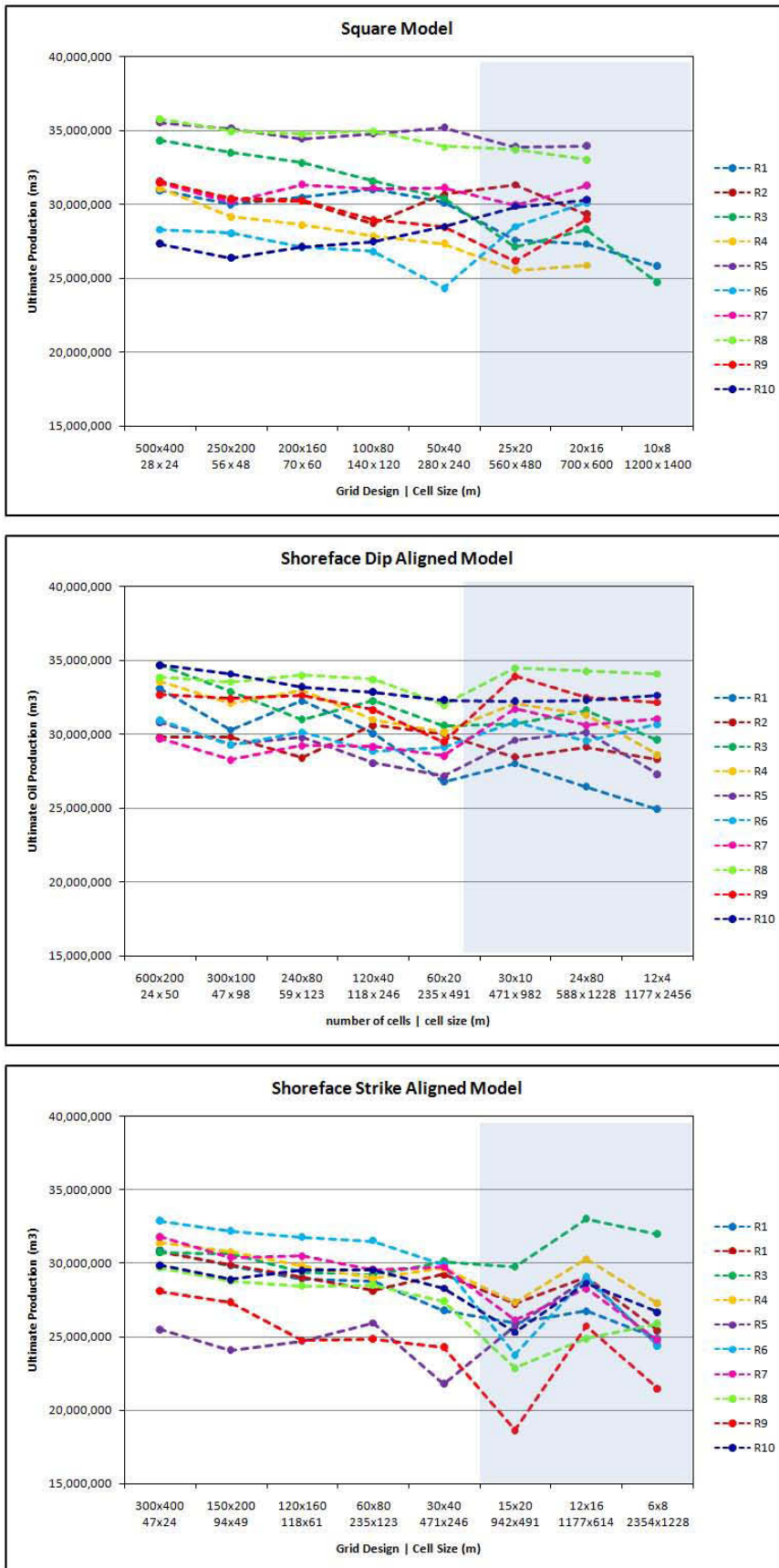
Figure 6.48. Total field oil production, 3-layer grids of the coast scenario - realizations 1–10. These three grid designs both show a similar total field production trends and spread of results for ten realizations. Many realizations have little variation as the grids are upscaled. Those that do show variation, generally vary by less than 10 percent of the total value of the previous grid.
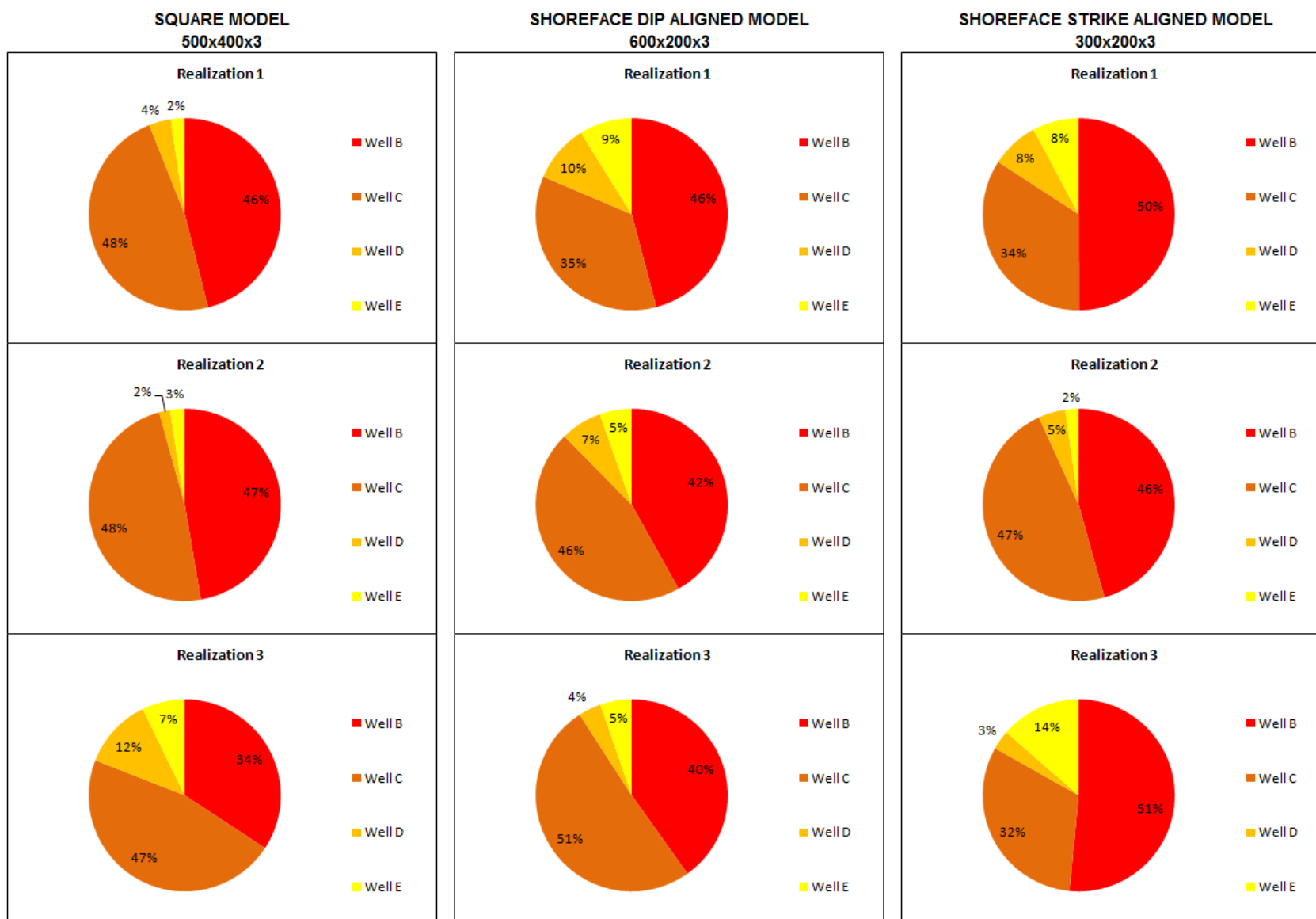
SQUARE MODEL
500x400x3

Realization 1, Realization 2, Realization 3

SHOREFACE DIP ALIGNED MODEL
600x200x3

Realization 1, Realization 2, Realization 3

SHOREFACE STRIKE ALIGNED MODEL
300x200x3

Realization 1, Realization 2, Realization 3

Figure 6.49. Square grid, coast scenario. A breakdown of the relative contribution to total field production of each well. This shows that Wells B and C are consistently the main contributors to production in the coast models and generally produce a similar amount.
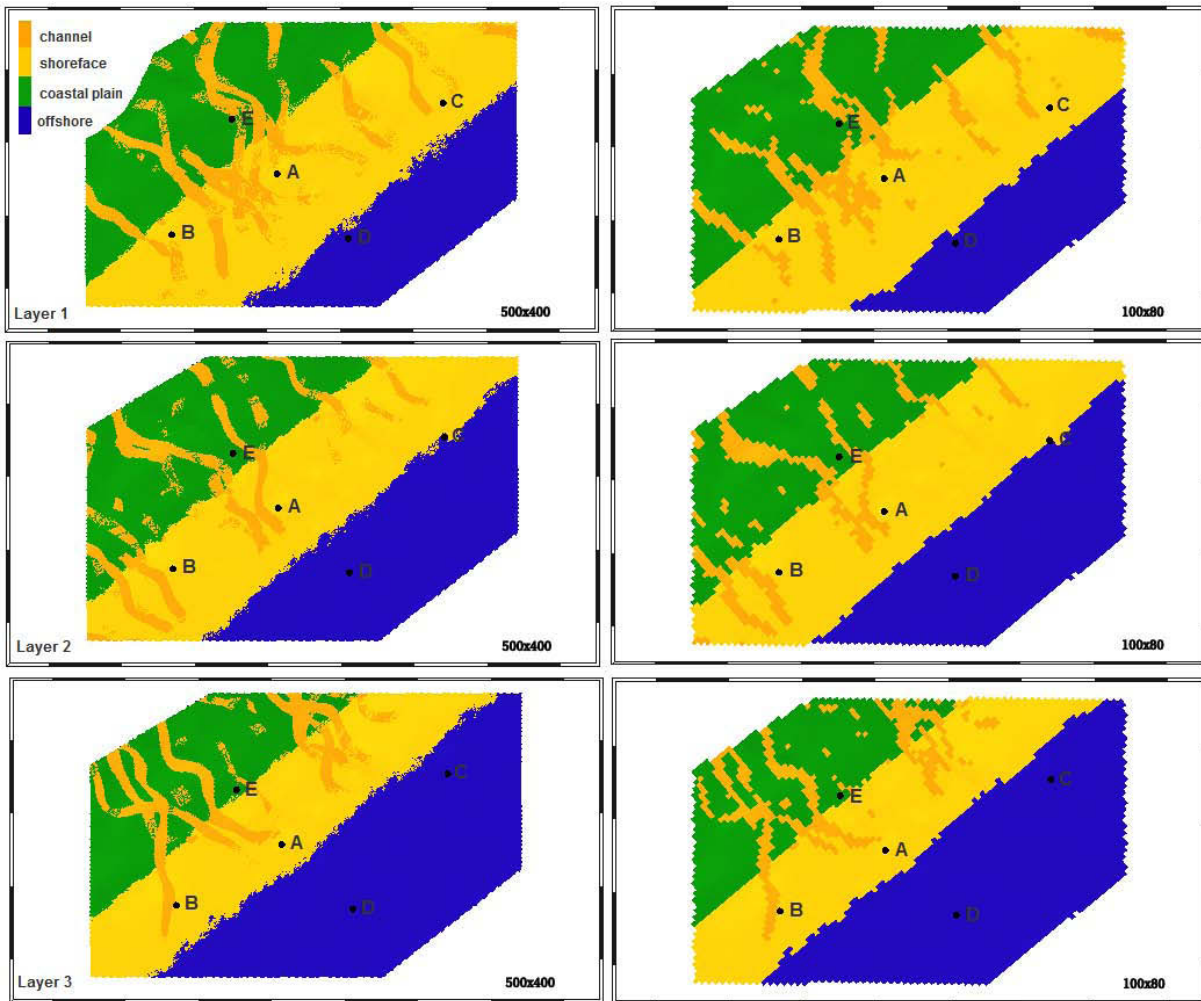
Figure 6.50. Facies model of coast scenario, square grid, Realization 1. This figure shows the facies distribution in the 3-layer grid. Wells A and B are always located in the shoreface zone, while well C penetrates the shoreface in the top layer (1) is close to the shoreface/offshore interface in layer 2 and which facies it penetrates varies between realizations and penetrates the offshore facies in layer 3 (base of model). Well D always penetrates the offshore facies. Well E is located on the coastal plain in layers 1 and 2, and is near the landward edge of the shoreface in layer 3 and in some realizations will be located in the shoreface facies. Well E may penetrate channels facies on the coastal plain while wells A, B and C may penetrate channel facies adjacent to shoreface facies.

The 100 x 80 grids (right) show that as the grids are horizontally upscaled the edges of the shoreface are smoothed and wells C and E may be affected by upscaling associated facies shift. In the square grid design the 50 x 40 grid is the last upscaling step to capture the any of the morphology of the shoreface boundary.
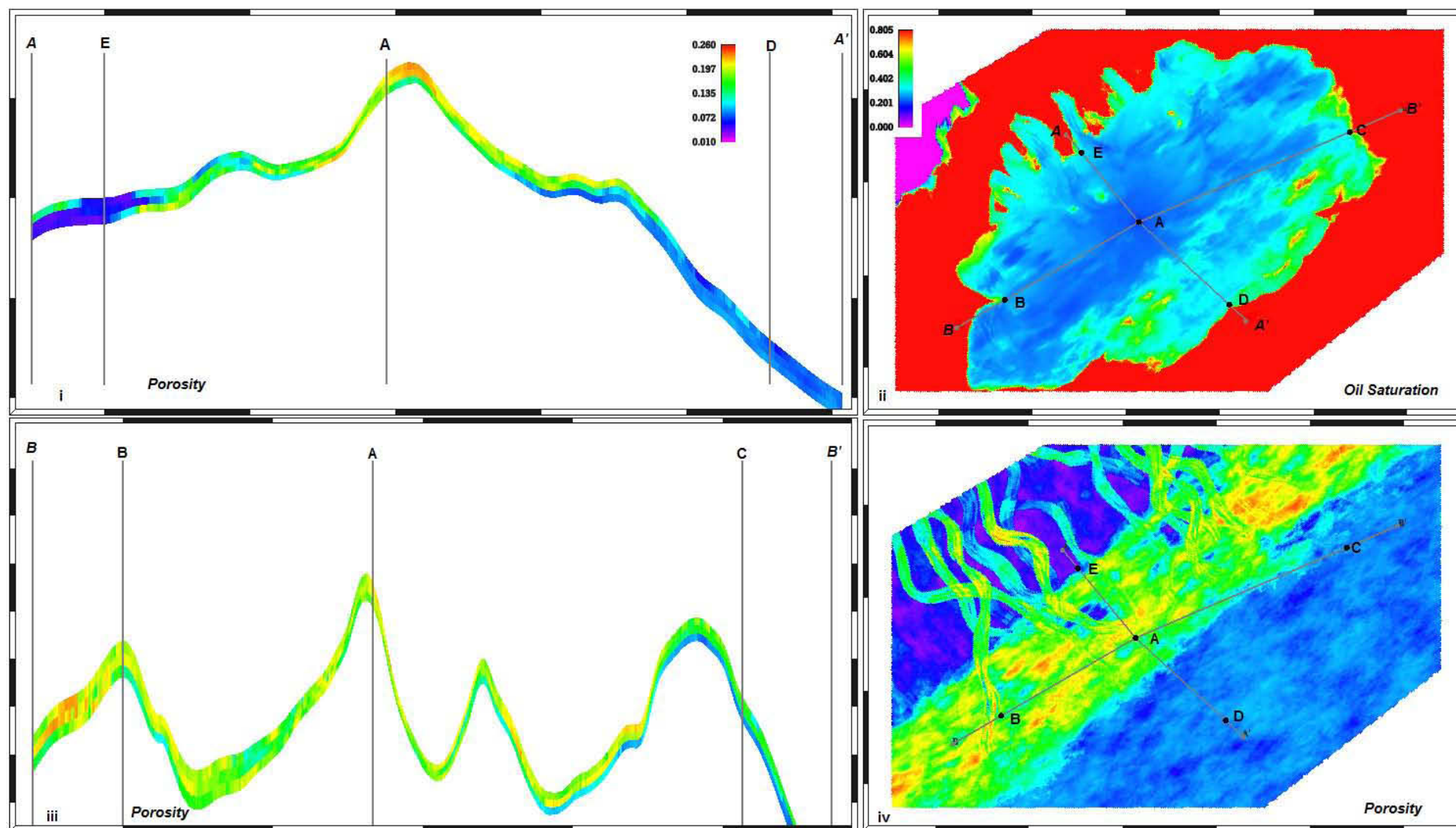
Figure 6.51. Coast scenario, SQ500 x 400 x 3 grid, Realization 1. This figure highlights the position of Wells E and D relative to the shoreface and channel facies (i). Well E is adjacent to a channel.
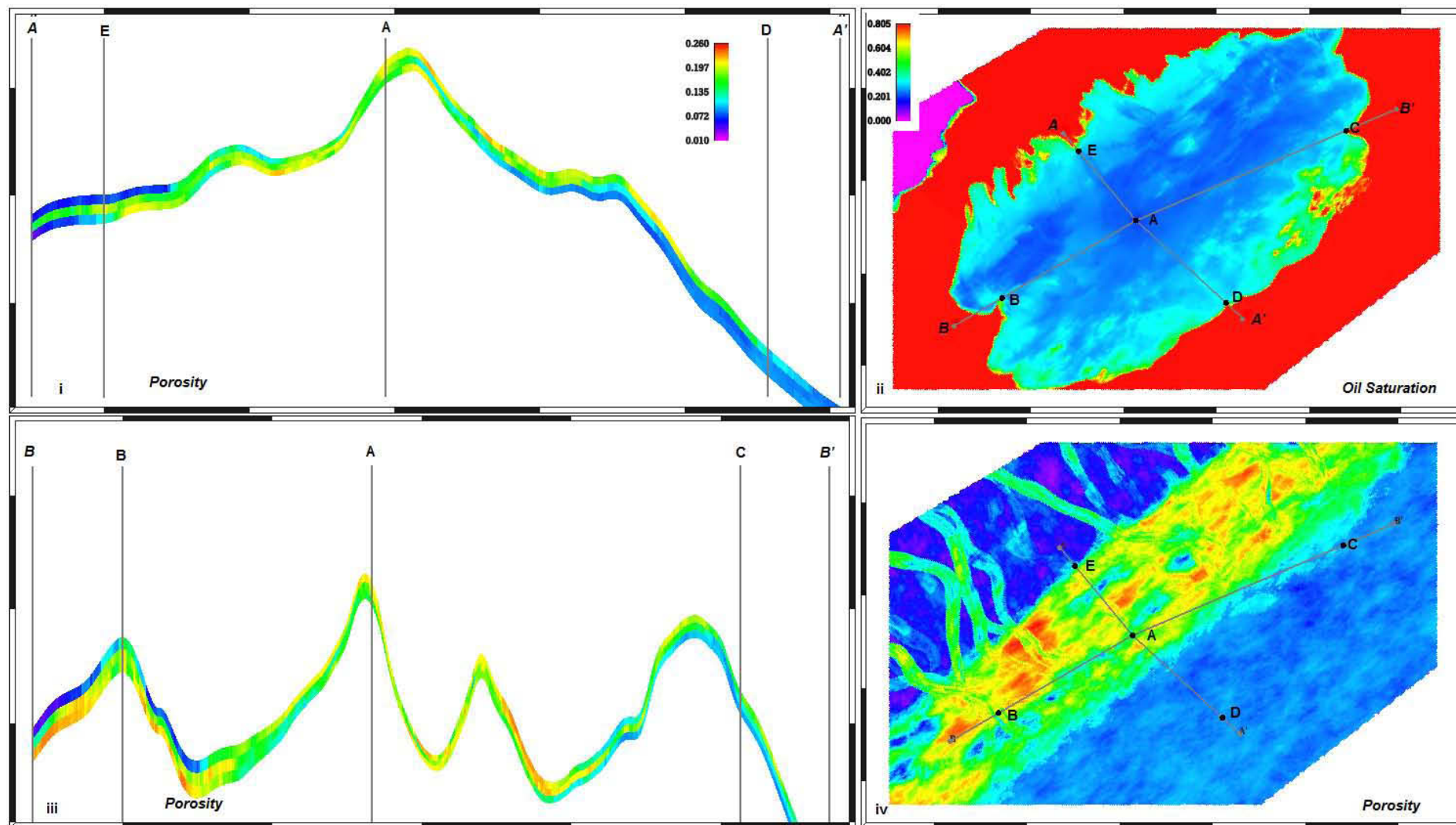
Figure 6.52. Coast scenario, SQ500 x 400 x 3 grid, Realization 3. In this scenario well E penetrates channel or shoreface facies in two layers of the well. As a result this well produces significantly more oil than realization 1 (Figure 6.51).
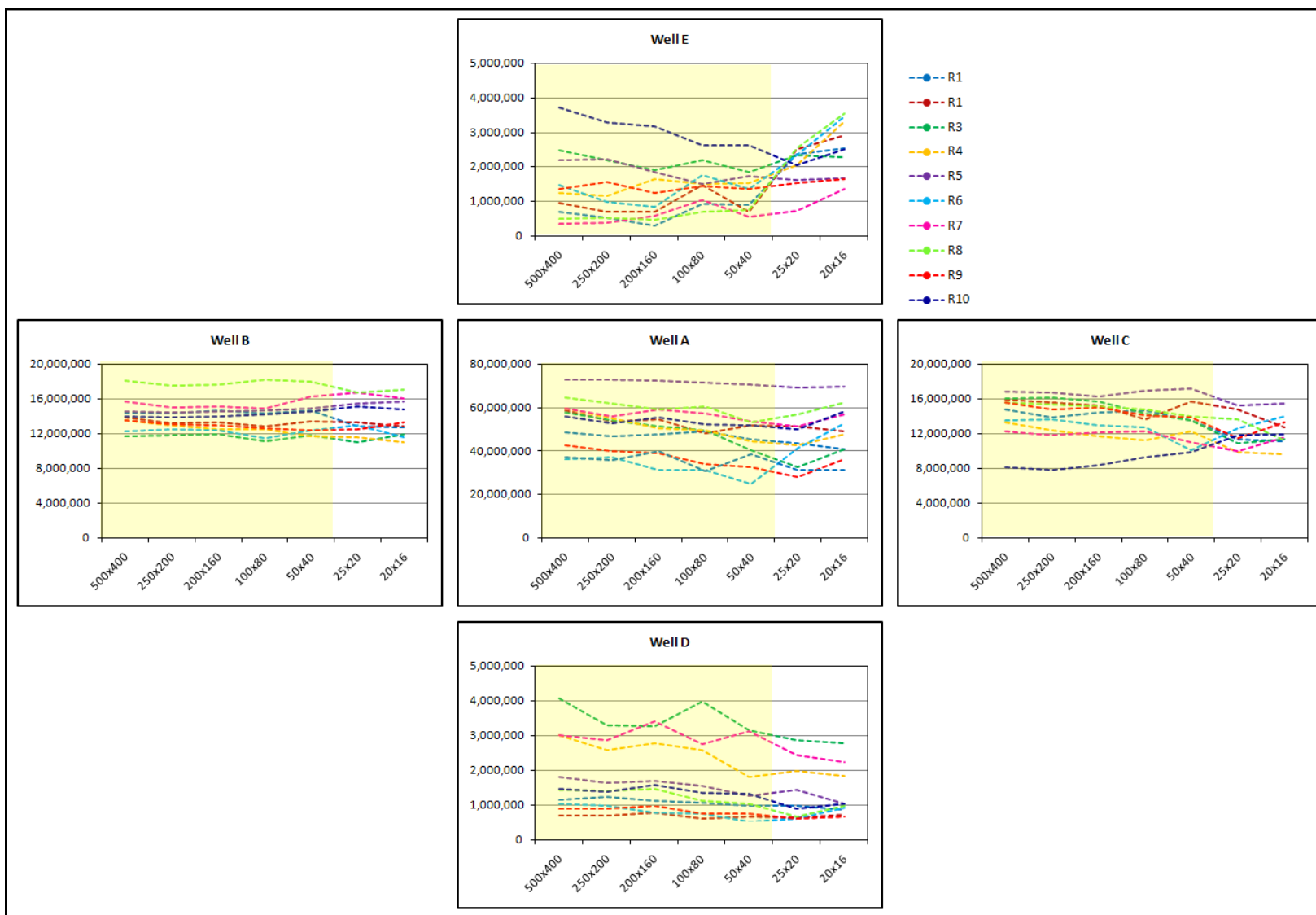
Figure 6.53 Ultimate production or injection for square grid coast scenario. The well with the greatest amount of variability between grids is Well E. This well is the most landward well and is located close to the edge of the shoreface. The realizations that produce the most in Well E penetrate a fluvial channel in at least one layer and/or penetrate the inside edge of the shoreface porosity instead of the outside edge in layer 3. Similarly, the realizations that produce the most from Well D penetrate the inside edge of the shoreface porosity in Layer 1 instead of the poorer quality outside edge.
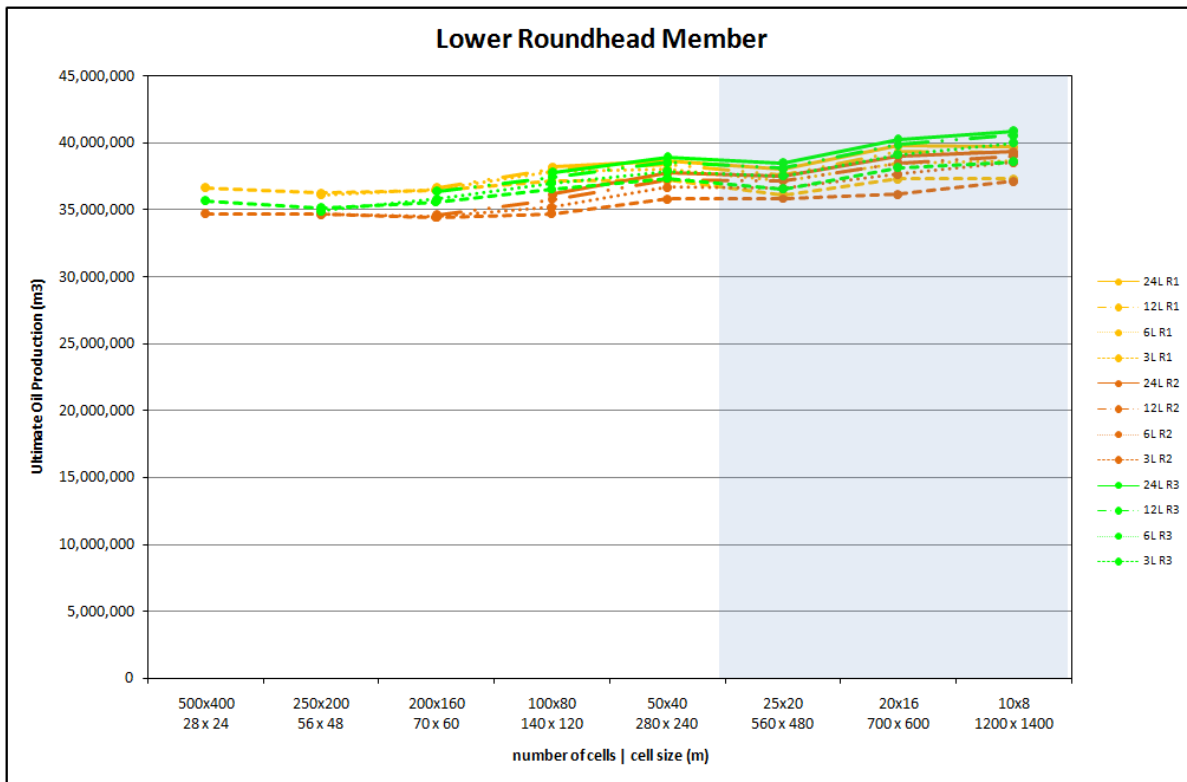
Figure 6.54. Ultimate oil production for lower Roundhead Member scenario. This model honours the data at the Flounder wells that penetrate this interval. The simulation injects and produces from the conceptual vertical wells only. These wells are very close to actual Flounder wells, thus the amount of variation in reservoir at the production locations is very limited.
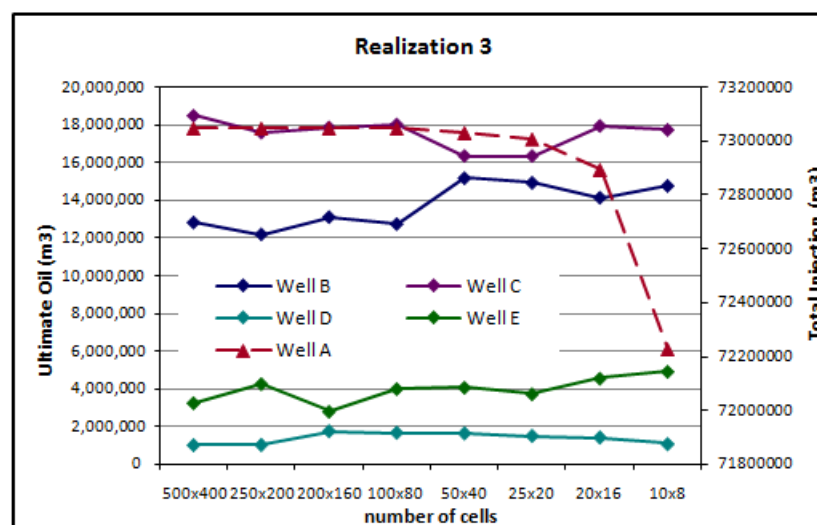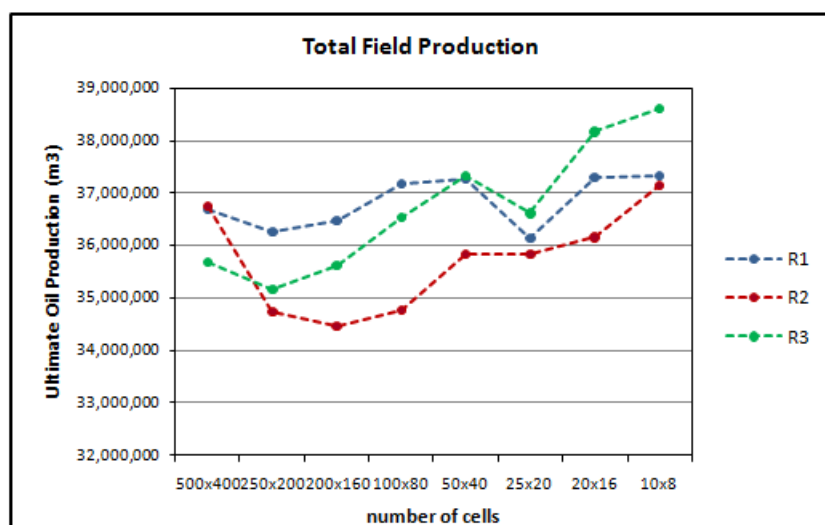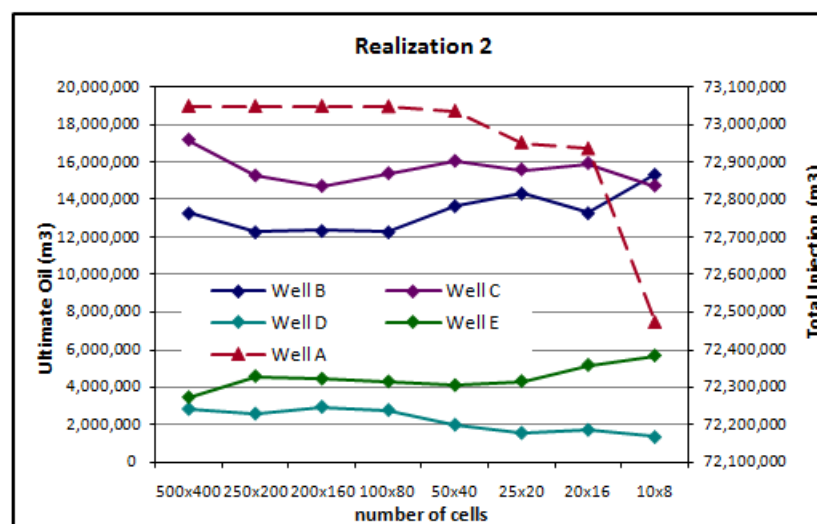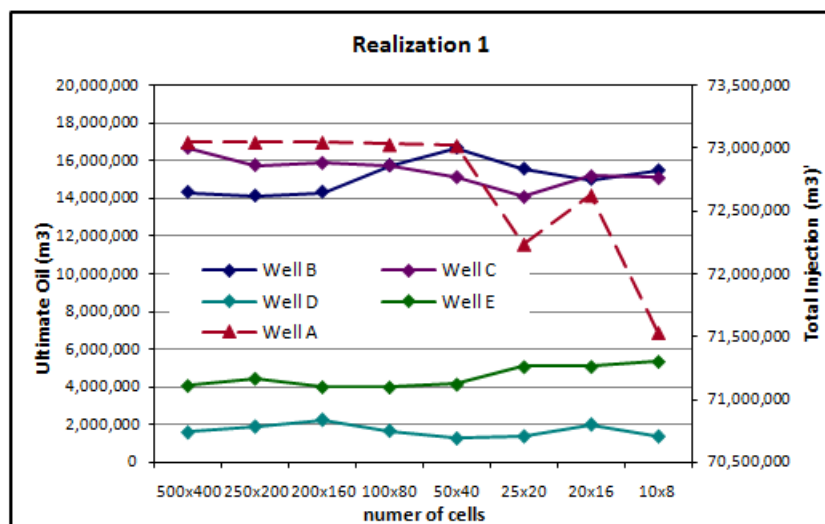
Figure 6.55. Ultimate oil production by well for the Lower Roundhead scenario, 3-layer grid designs. Realizations 1 and 2 have a very similar total production for the 500 x 400 grid, the individual well production is quite different. Well B penetrates channel facies in all layers, and has an increase in production between the 100 x 80 grid and the 50 x 40 grid (the point at which cell width exceeds channel width). This suggests that the presence of channel facies in this well is influencing how production changes with upscaling.
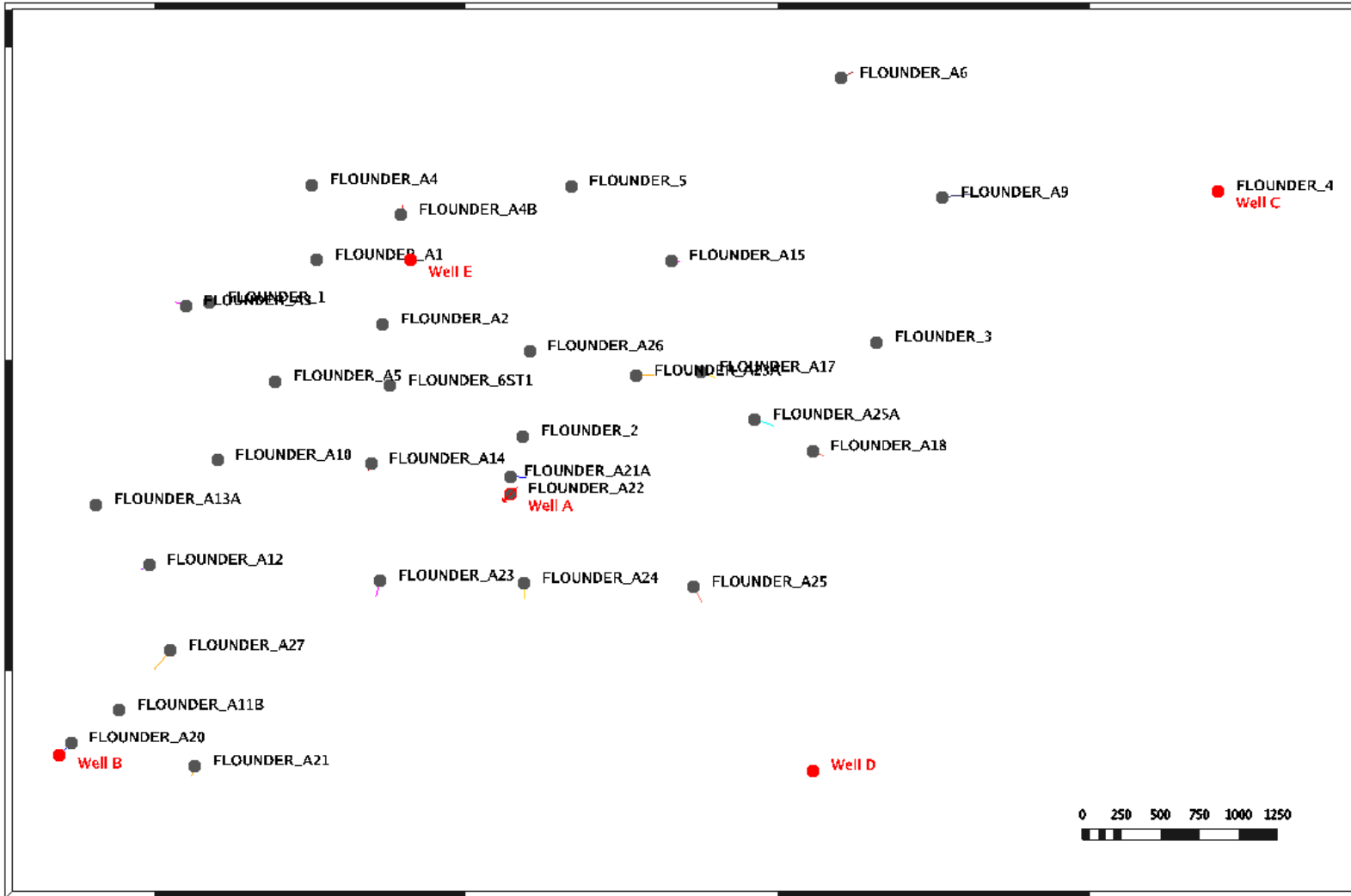
Figure 6.56. Base map showing the actual Flounder Field wells and the conceptual vertical wells (red) used for reservoir simulation. The distribution of facies and porosity was tied to the actual wells (black) in the 1st generation models such as the lower Roundhead model.
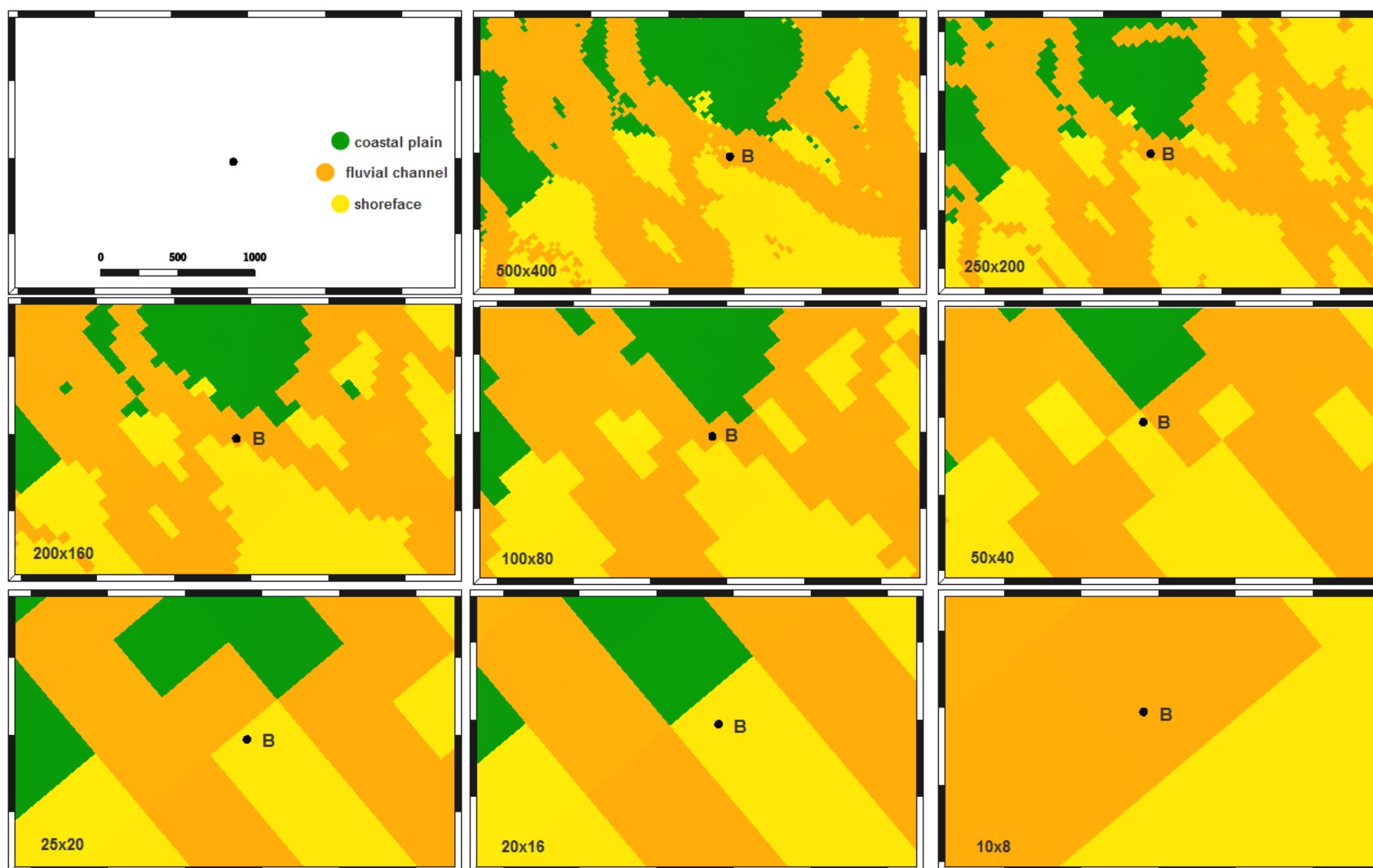
Figure 6.57. Facies model of the lower Roundhead Member around Well B. Realization 3, layer 3. Well B penetrates channel facies in all three layers of the model. In this realization, the width of the channel that Well B penetrates is approximately equal to the cell size of the 100 x 80 model.
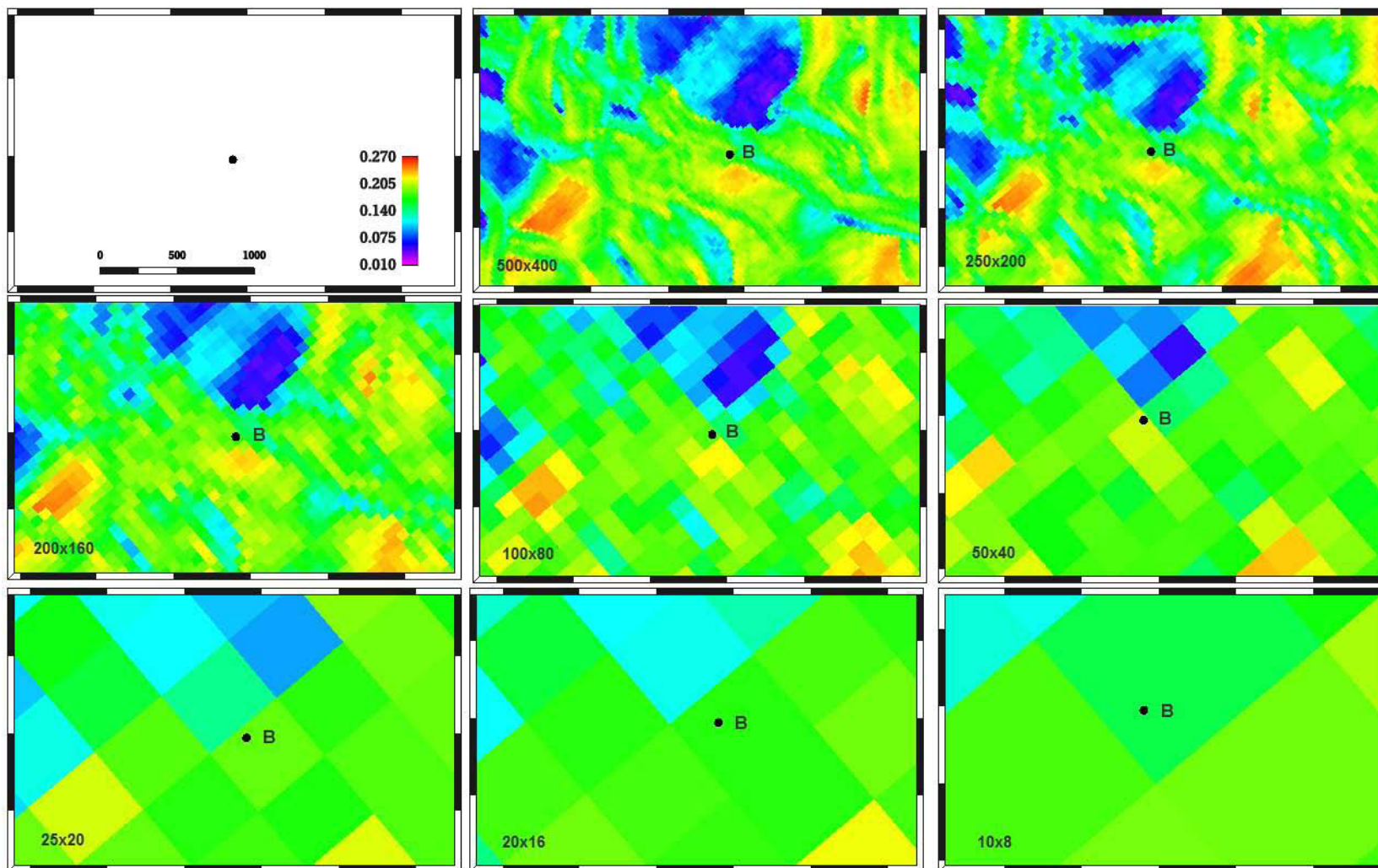
Figure 6.58. Porosity model, lower Roundhead Member model. Realization 3, layer 3—detail around Well B. Figure 6.57 showed that the facies at Well B changes from channel to shoreface in the 50 x 80 grid. In the porosity model it can be seen that the porosity increases in the 50 x 80 grid. As a result, the permeability in this layer at the wellbore changes from 274 mD/m to 1479 mD/m.
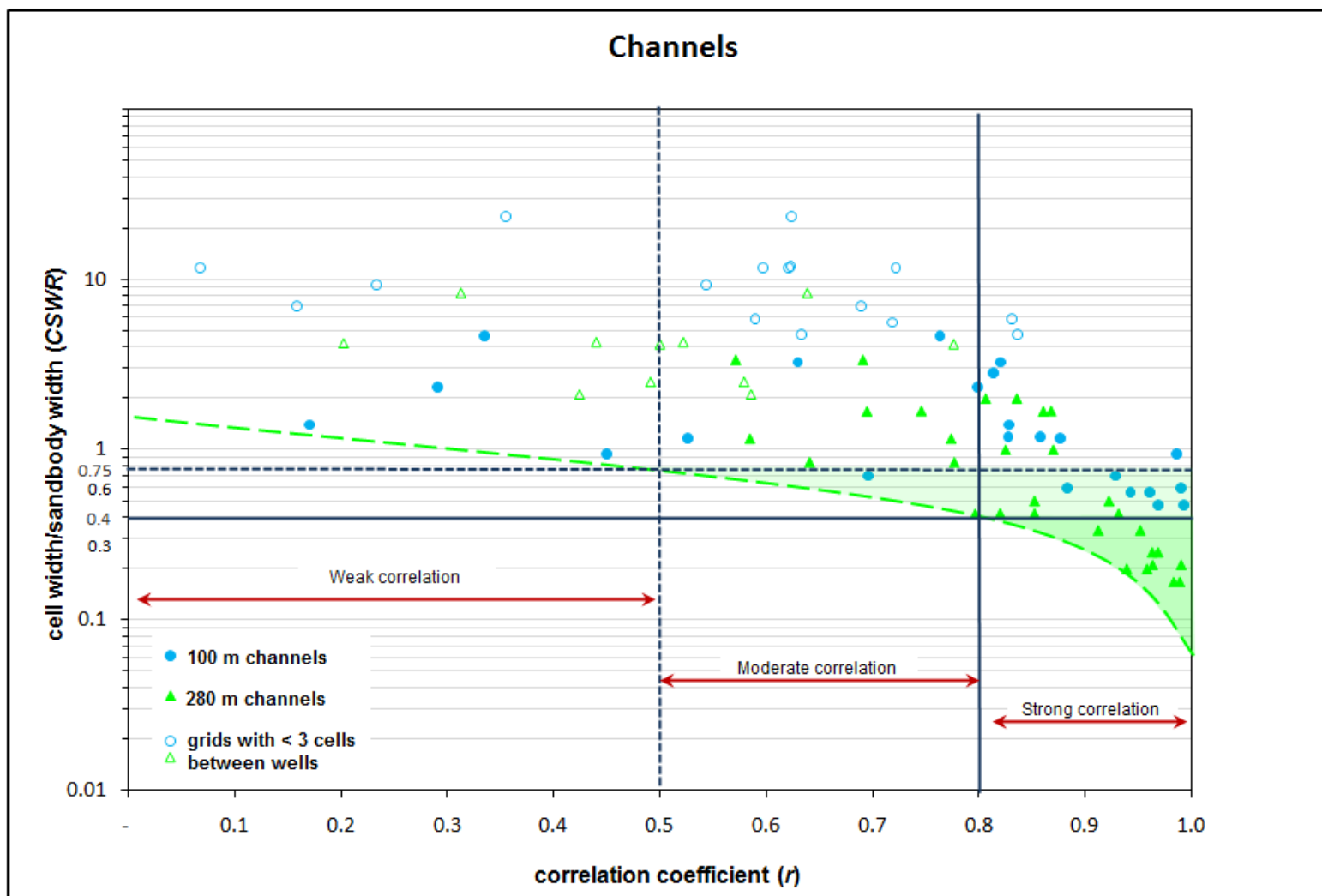
Figure 6.59. Correlation coefficient (r) of base grid production and upscaled grid production versus cell-width to sandbody-width ratio (CSWR). Channel scenarios. This chart highlights that once the cell width is greater than 0.4 times the channel width there is a decreasing chance of a correlation between the ultimate production of the base grid and that of the upscaled grids. A correlation is considered strong if 0.8≤r≤1 (dark green shaded area) and weak when r is ≤ 0.5.
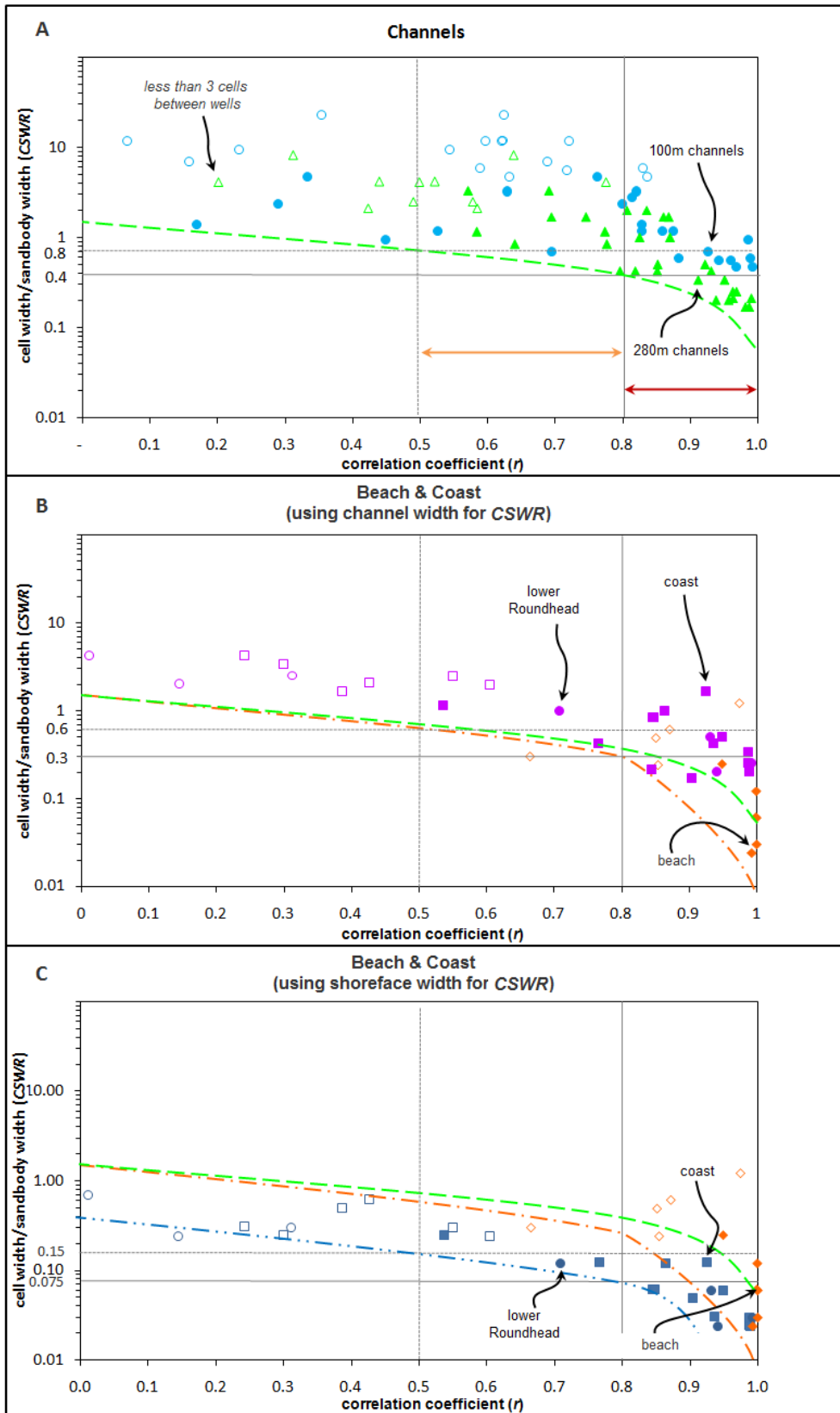
Figure 6.60. A comparison of the relationship between correlation coefficient and CSWR for the scenarios modelled. The CSWR of the coast and lower Roundhead scenarios could be related to either the channel width (B) or the width of the shoreface (C). The plots (B and C) suggest that the data fits the pattern established by the channel and beach scenarios best if the CSWR for the channel facies is used rather than the shoreface facies (B). This indicates that the channels are having an impact on the simulation results, even if it is not visually obvious.
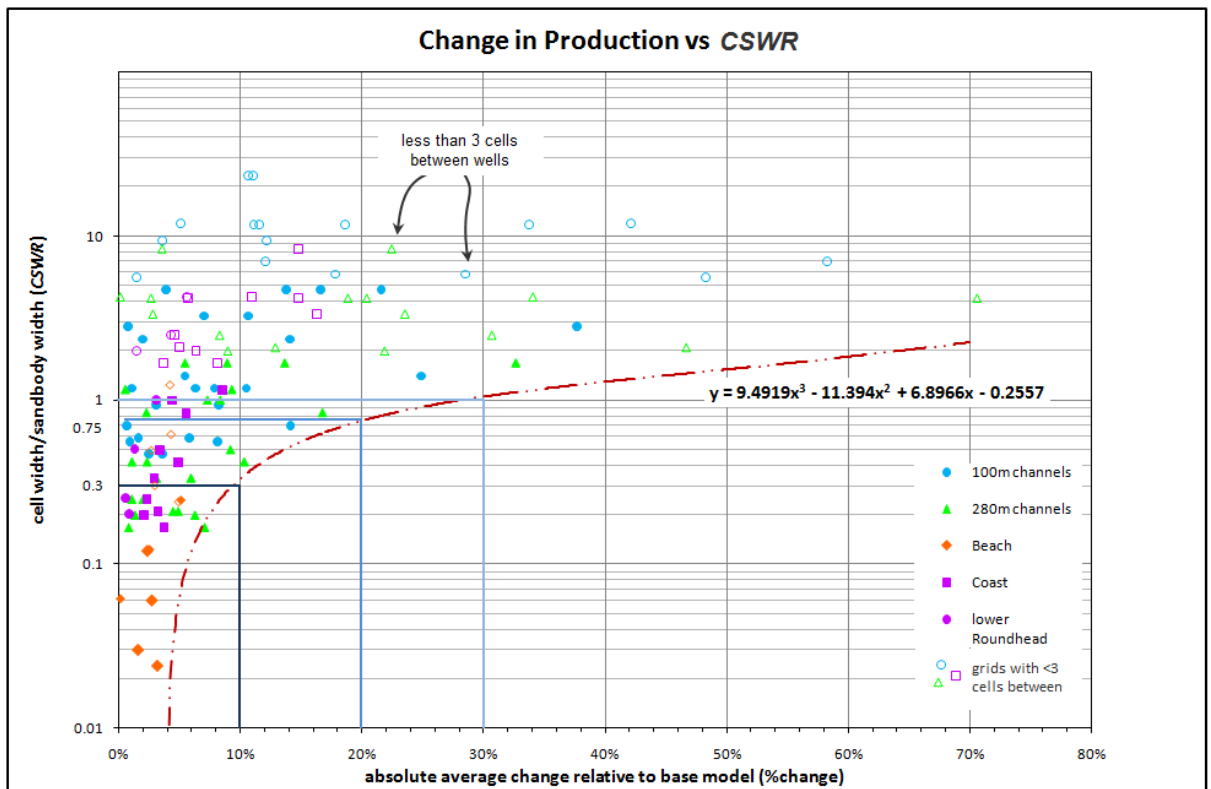
Figure 6.61. %change vs. CSWR for all scenarios. The red line denotes the maximum expected change in ultimate production for any given CSWR. This dataset indicates that up to 4% difference can always be expected. When the CSWR is less than 0.3 (the cut-off for *r* always being greater than 0.8; Figure 6.60) there is less than 10% difference between the upscaled grid and the base grid. When CSWR is 0.75 (r=0.5:Figure 6.60), the amount of variation could be up to 20%-though the majority of results are less than 10%. When the CSWR is greater than 1, %change can be as much as 70%, with a much greater spread of results than was seen when the CSWR is less than 1.
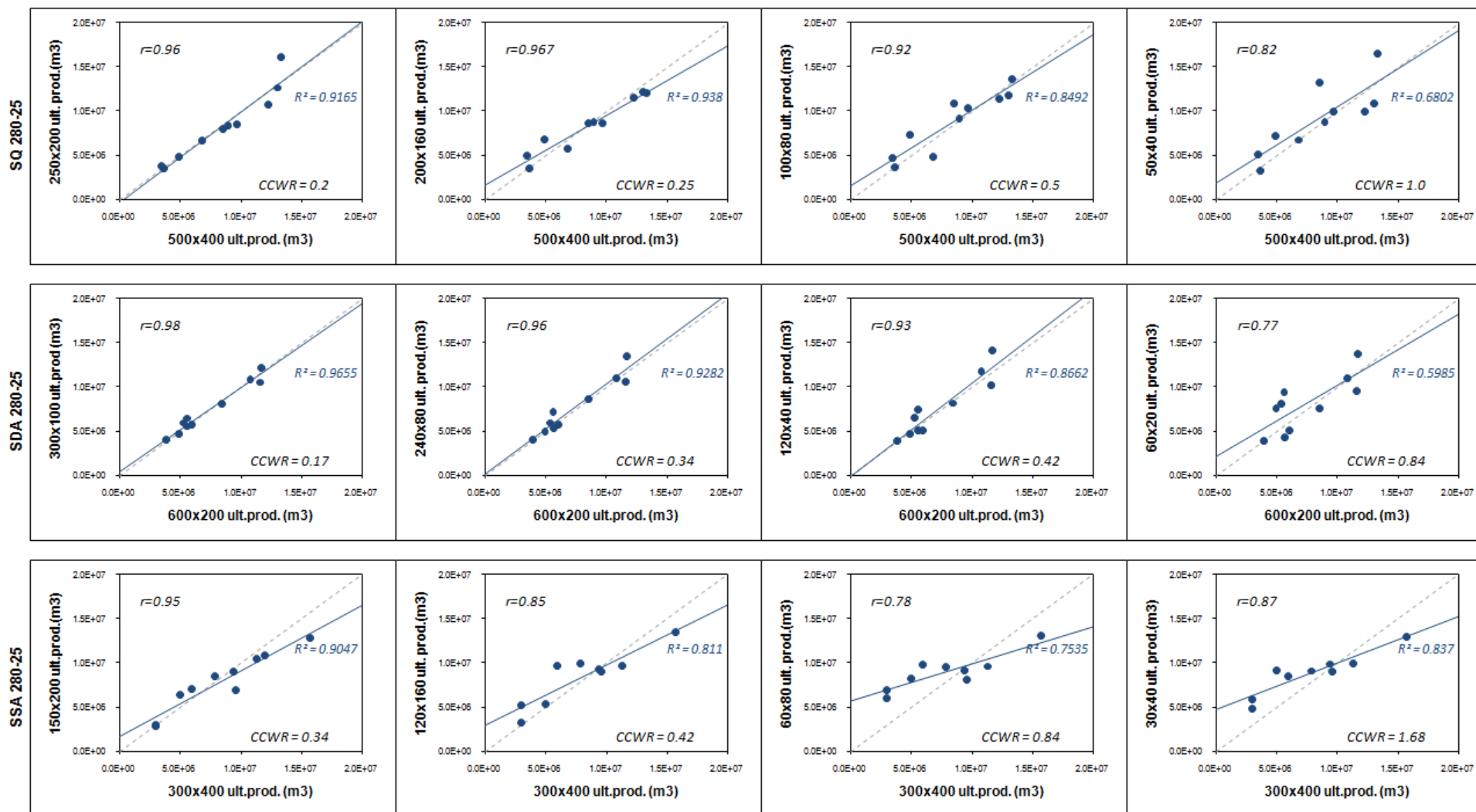
Figure 6.62. Production from base grid vs. production from upscaled grids. 280-25 scenario. These charts indicate that as the grids are upscaled there is an increasing tendency to overestimate production for realizations with relatively low recovery and overestimate it for wells with high production. When the CSWR exceeds 0.3 there is an increasing scatter of results, though there are always some that remain close to the 1:1 gradient (grey line).
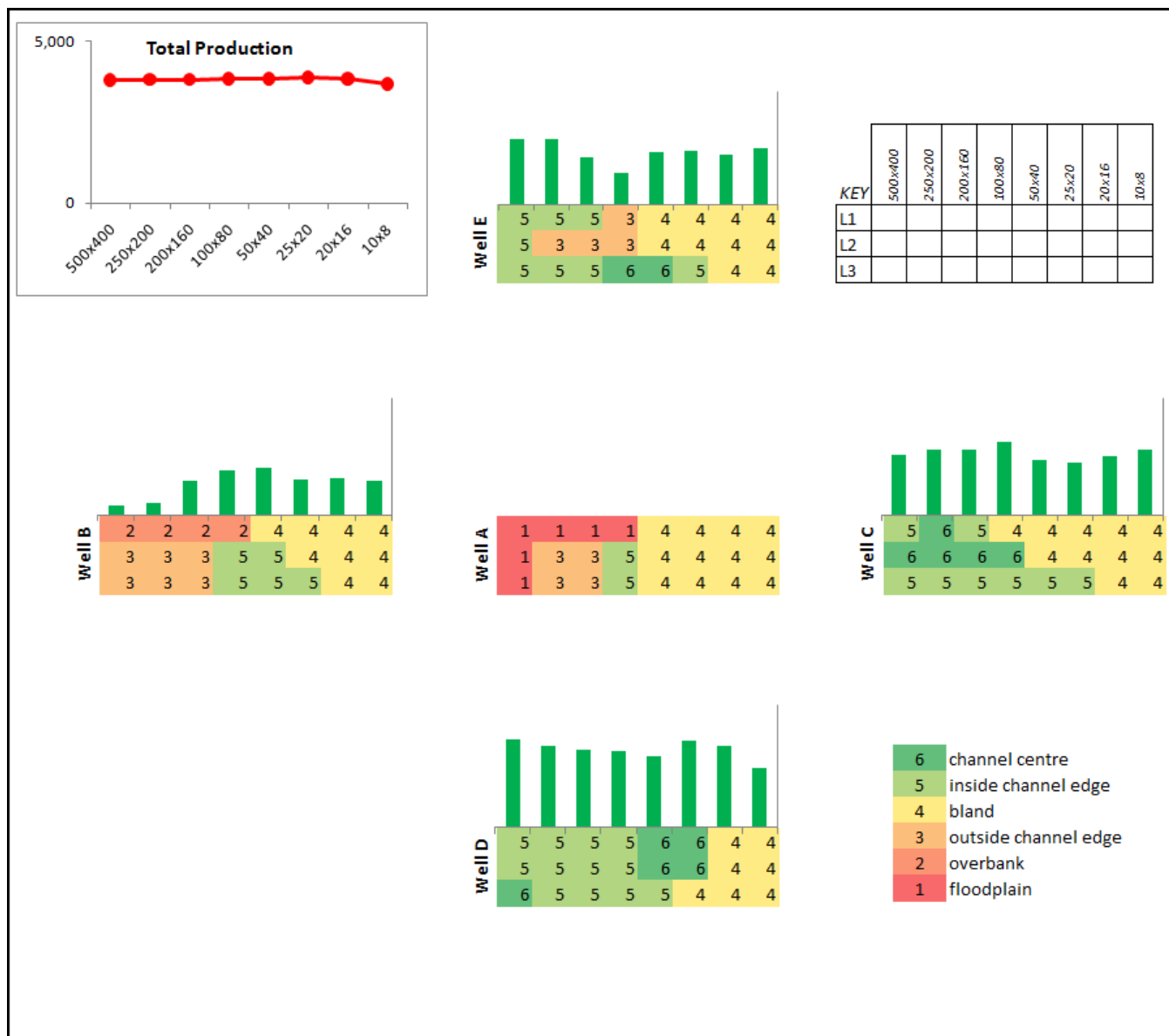
Figure 6.63. Realization 9, SQ100-25 scenario. No injection. This figure shows the influence of channel position on production and upscaling when injection is not taking place. Well B is located close to a channel, and its productivity changes significantly once the grids are upscaled beyond the width of the channels. Well C, which penetrates a channel in several layers, looses production as the grids are upscaled and porosity distribution is smoothed. This is in contrast with the wells behaviour when injection is taking place at Well A (Figure 6.29). In that case, the production profile of Well C reflects the injection profile of Well A. and increases as the grids are upscaled.
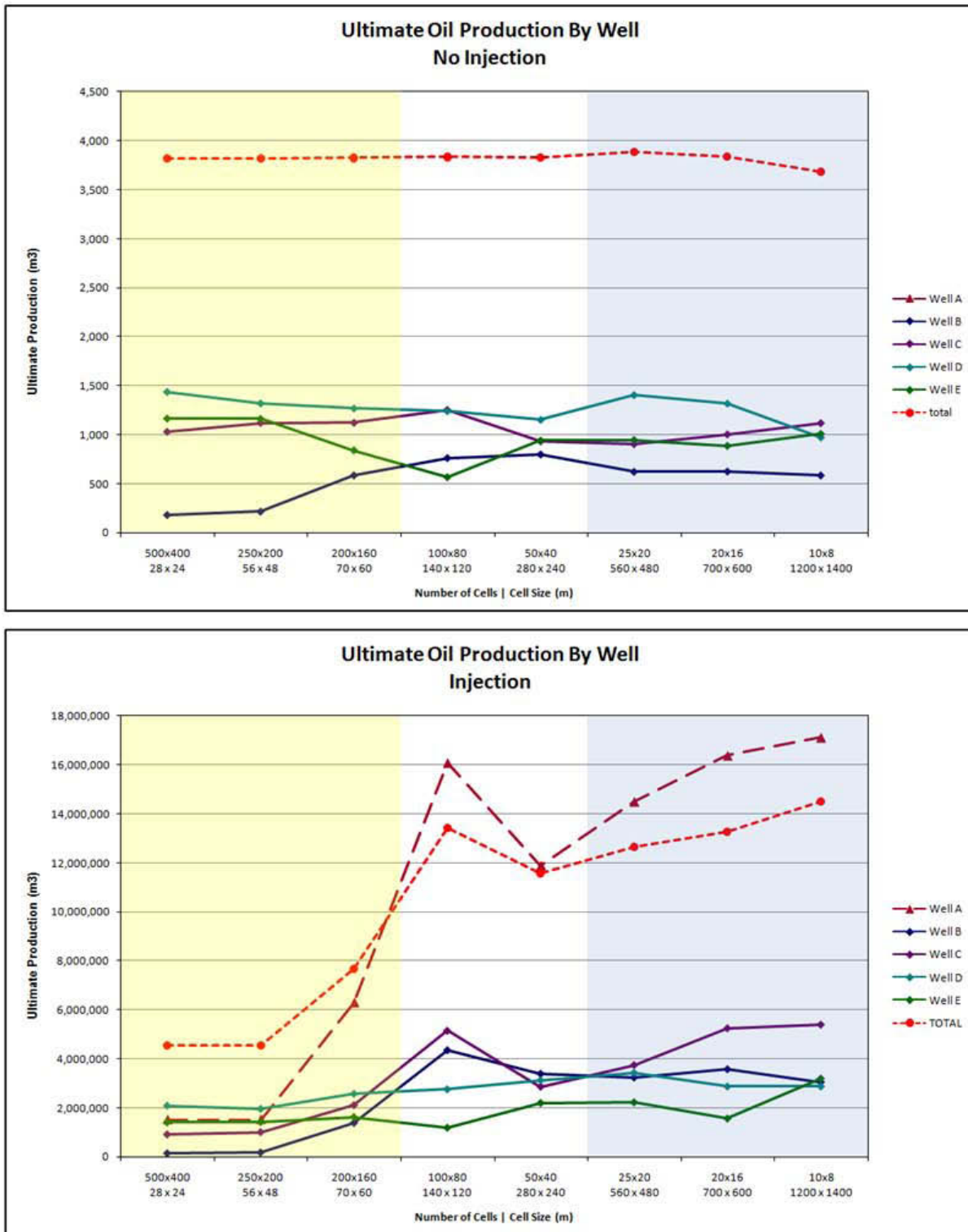
Figure 6.64. Realization 9, SQ100-25 scenario. A comparison of well performances with and without water injection at Well A. When injection is not taking place the total field production is relatively constant across all grid sizes. When injection is performed, the production profile reflects the fact that the injector is in a poor reservoir quality area, and the benefit of injection is only seen once the grids are upscaled to a point that the porosity distribution around the well locations has been significantly altered.
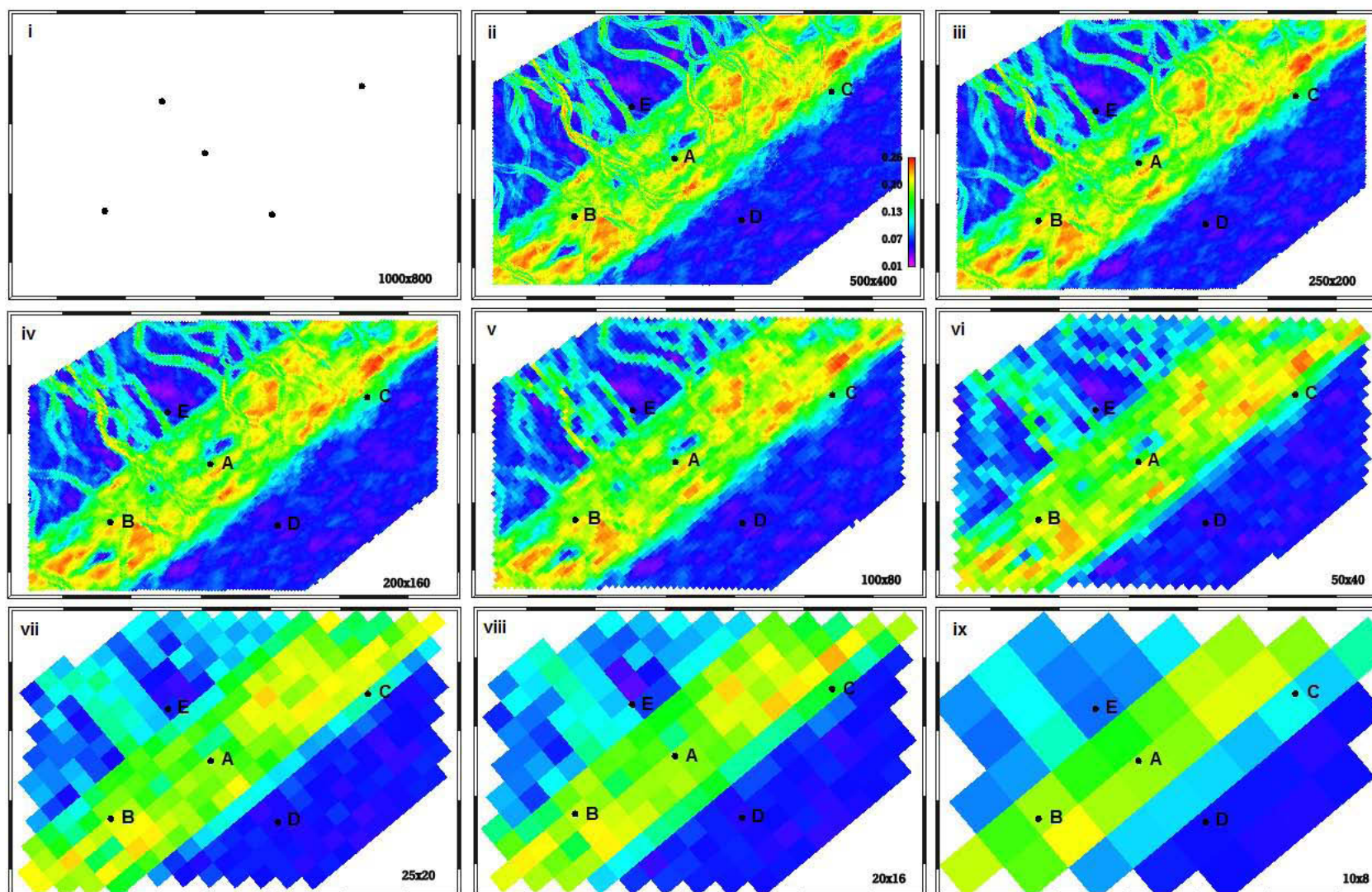
Figure 6.65. Coast scenario porosity grids - Realization 6, square grid. The channels are identifiable within the shoreface facies by their different orientation of porosity streaks (ii). The channels are 280 m wide, and are the same width as the cells in the 50 x 40 grid (vi)—at which point they are no longer identifiable in the shoreface facies. Channel morphology and connectivity in the coastal plain is retained up to the 100 x 80 grids—which have cells half the width of the channels.
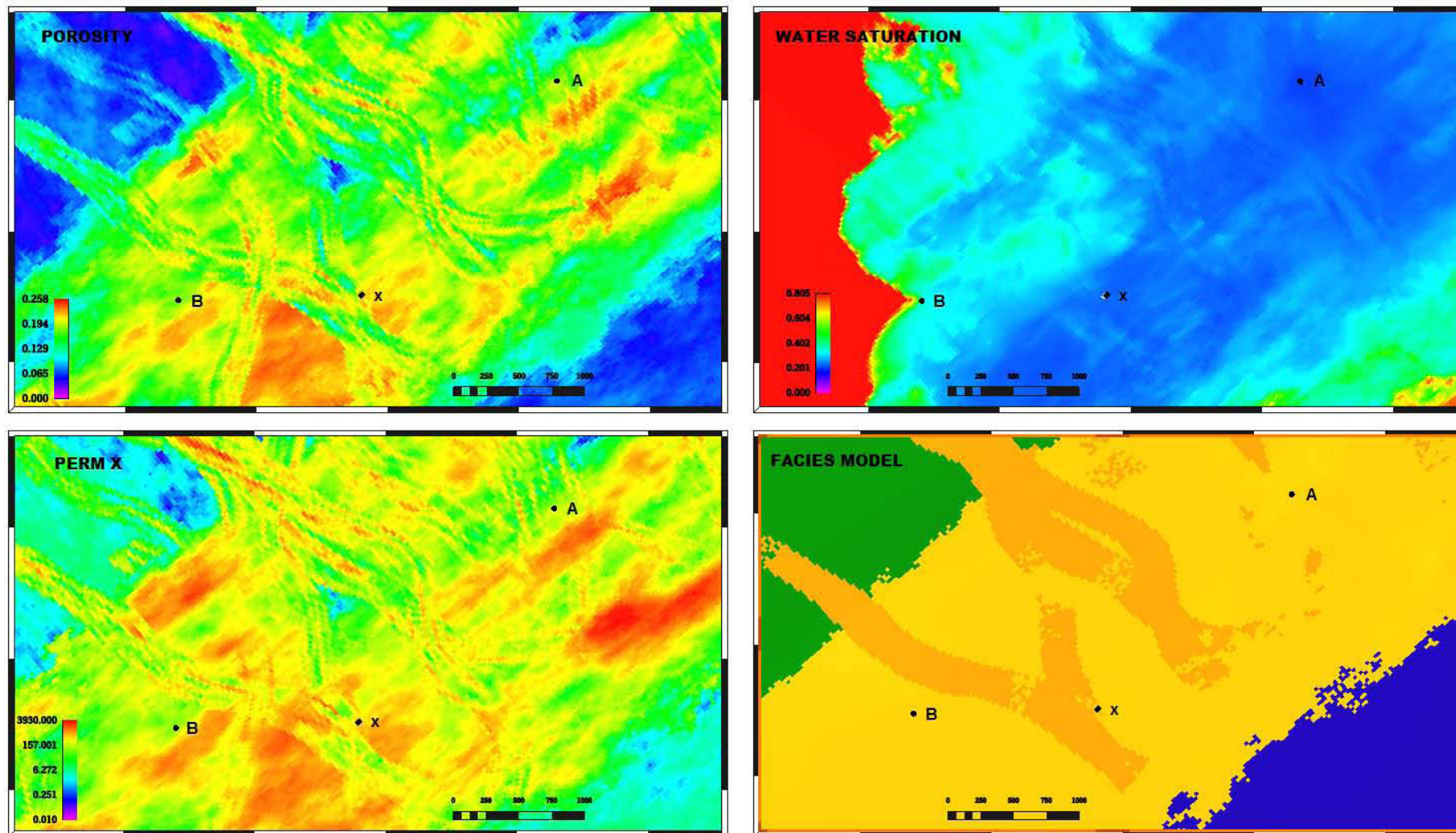
Figure 6.66. Detail of models and water injection pathways—Realization 6, Layer 2. 500 x 400 x 3 grid. Numerous channels can be seen in the shoreface in the porosity and permeability models between wells A and B. These cause subtle changes in the water saturation model. The x mark highlights the edge of a channel which is stands out in the facies, porosity and permeability models, but much less distinct in the water saturation model.
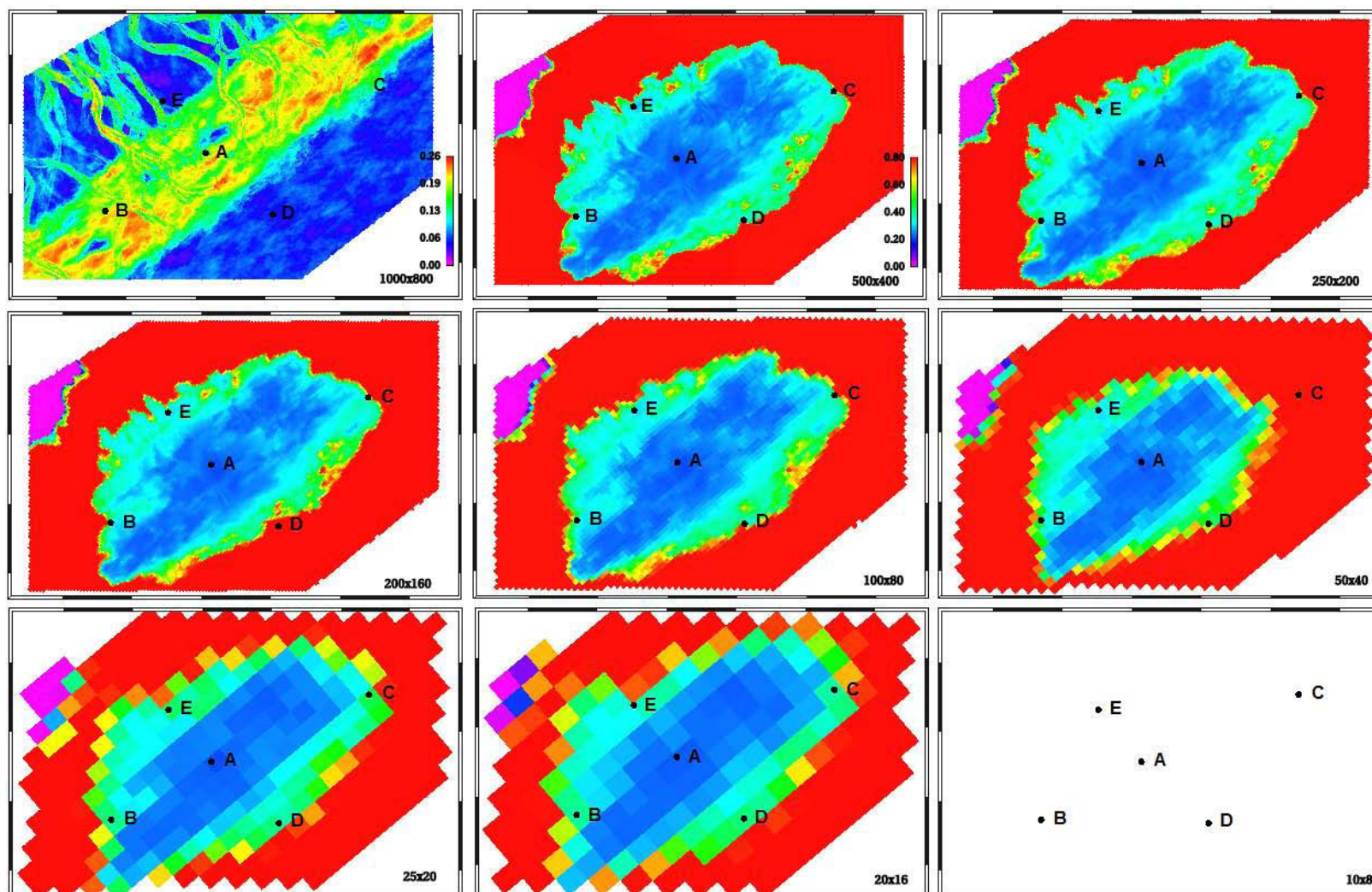
Figure 6.67. Water saturation at 20 years, layer 2 of coast model, Realization 6. This shows the common water influx pattern in this scenario. The majority of water moves along strike to wells B and C. Water influx into the coastal plain facies follows channel paths—see area to the west of well E. Wells D and C, on the edge of the water influx are most affected by upscaling induced changes. The influence of the channel facies within the shoreface is subtle, but can be seen in the 500 x 400, 250 x 200 and 200 x 160 grids. It cannot be seen in the 100 x 80 grid—which is where the cell size equals the half the channel width.
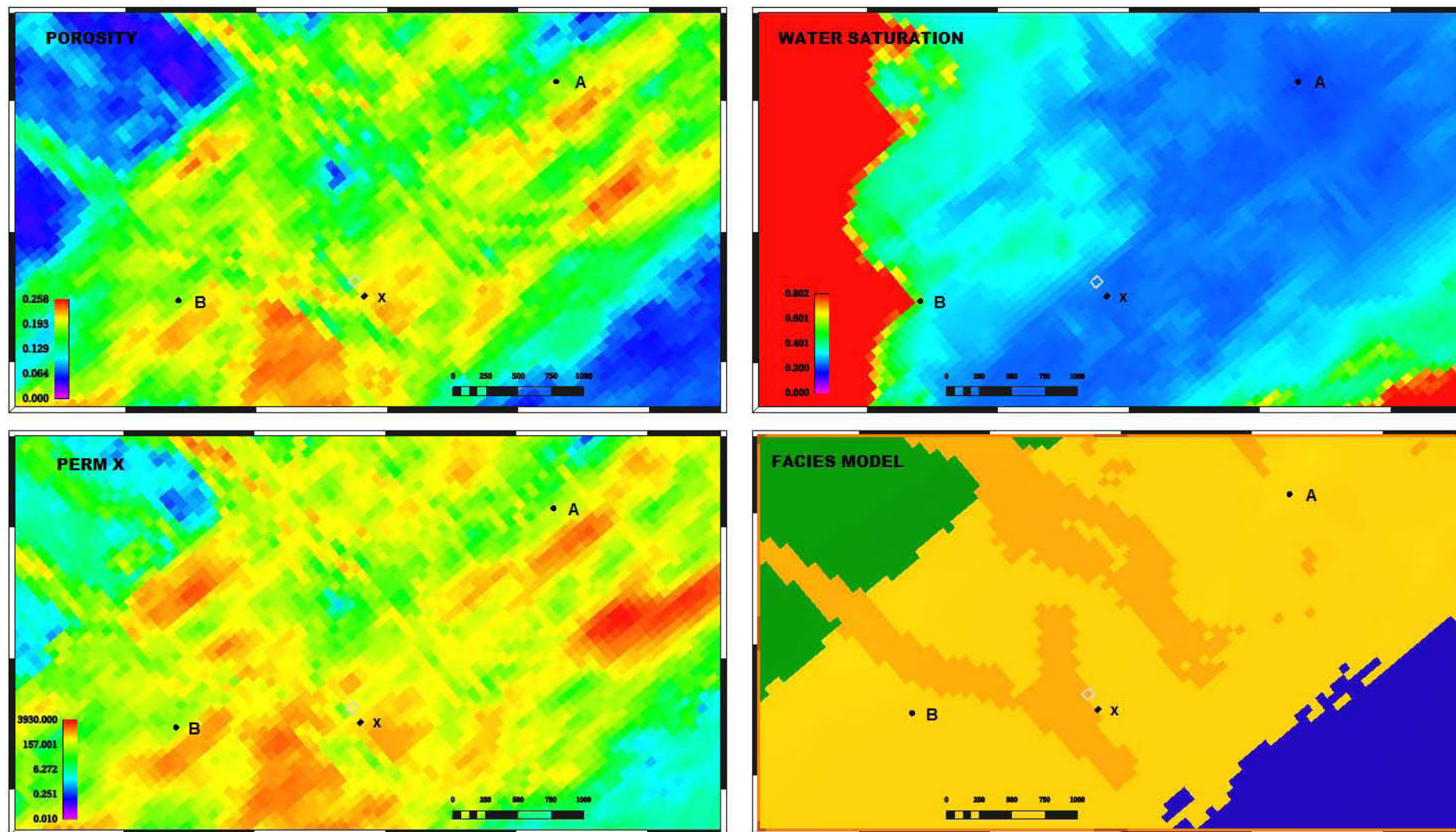
Figure 6.68. Detail of models and water injection pathways—Realization 6, Layer 2. 200 x 160 x 3 grid. Although the channel near the 'x' mark is still visible—particularly in the facies and porosity grids—its influence on the water injection patterns is no longer recognizable.